Integrated Hybrid AI–GIS Framework for Temperature-Driven Drought Early Warning and Agricultural Risk Mapping in Bangladesh

Hasan Ahamed Alif[1], Md. Jisan Mashrafi[2], Sudoy Kumer Ghosh[3]

[1]*Department of Computer Science and Engineering, Dhaanish Ahmed College of Engineering, Affiliated to Anna University, Chennai – 601301, India*

[2]*Department of Computer Science and Engineering, BRAC University, Dhaka, Bangladesh*

[3]*Department of Electrical and Electronics Engineering, Dhaanish Ahmed College of Engineering, Affiliated to Anna University, Chennai – 601301, India*

***Corresponding author:** md.jisan.mashrafi@g.bracu.ac.bd

Abstract

Drought has also become a potential threat of growing severity to agricultural sustainability and food security in climate-sensitive areas of South Asia. In Bangladesh, recurring and escalating episodes of drought in northwestern drought-prone areas, especially the Rajshahi district, have been caused by continuous heat-related stress, extended dry season, and changes in surface energy balance. In this research, an artificial intelligence-geospatial model is established to predict long-term temperature changes, measure spatial heat stress, and assess the agricultural risk posed by drought in the Rajshahi district. The ten hybrid forecasting models (LSTM, GRU, CNN, Informer, ARIMA, and ANFIS) that can combine both advanced signal decomposition methods (CEEMDAN, wavelet transform, variational mode decomposition, and STL) with deep learning and statistical learners were trained on a total of more than four decades (1980-2024) of monthly temperature records of the Bangladesh Meteorological Department (BMD). The results of the model performance were measured through various statistical values (MAE, RMSE, MSE, and R 2) and the temperature projections were made until 2034. At the same time, land surface temperature (LST) data of Landsat multi-decadal (1984-2024) was also run on Google Earth Engine to evaluate the spatiotemporal changes in warming. Findings indicate that warming has exhibited a statistically significant, constant trend, accompanied by a significant increase in high-temperature anomalies. The highest predictive accuracy models (RMSE < 0.12°C, R^2> 0.99) were Wavelet-CNN-LSTM and CEEMDAN-SARIMA-CNN, while the remaining models, STL-ARIMA-BiLSTM and VMD-GRU-LSTM, also demonstrated good results (R^2> 0.99). Transformer-based and shallow hybrid designs, on the other hand, had low reliability in long-term temperature prediction. Spatial LST analysis reveals a progressive growth and intensification of thermal hotspots, particularly in western and southern agricultural regions, indicating continued surface heating and a decline in thermal buffering ability. Clusters of high similarity between the predictions and actual patterns of surface warming contribute to the high risk of drought-prone agricultural areas and the growing stresses due to heat. In general, the suggested AI-GIS framework proposes a powerful, scalable system for drought early warning, agricultural risk mapping, and climate adaptation planning, delivering actionable information to support irrigation management and sustainable agriculture in Bangladesh and other climate-prone areas.

Keywords: Drought early warning; Hybrid machine learning; Land surface temperature; Climate change; Agricultural risk; Bangladesh

1. Introduction

One of the most challenging and harmful climate-associated risks is drought that causes severe risks to agricultural sustainability, water security, and food systems in all the global regions (Mishra et al., 2023). Drought is not sudden and usually does not show itself until its effects become devastating, and the results of drought include failure of crops, water scarcity, and social and economic pressure (Mansouri et al., 2022). During the past decades, global climate change has been increasing the drought risk by raising temperatures on the surface, extending dryness, and changing the relationships between land and atmosphere in terms of energy (Zellou & Moçayd, 2023). These transformations are especially important to agrarian economies in South Asia, the livelihoods of which are directly associated with climate sensitive agricultural systems (Pokhariyal & Patel, 2023). Historically, Bangladesh is a country that experiences frequent droughts, although in the northwestern part of the country, the climate is monsoon-driven (Ayadi

& Forouheshfar, 2025). The area including Rajshahi district has a relatively low amount of rainfall, it has a high demand of evapotranspiration, and often, it is exposed to hot and dry winds (Guo & He, 2024). There are numerous incidents of severe droughts recorded in the historical records since the 1970s, most of which caused significant losses in rice and wheat production, water shortage, and food insecurity (Biazar & Golmohammadi, 2025). Such repetitive instances emphasize the weakness of the northwestern region of Bangladesh in terms of drought vulnerability and the necessity to develop a better drought risk assessment system and early-warning system (Han & Liu, 2024). Previous research on drought in Bangladesh depended mainly on historical data on rainfall variability, drought measures (including SPI and PDSI) and post-incident evaluation of agricultural damage (Mokhtar & Jalali, 2021). Although these methods were useful in understanding the historical instances of droughts, most of them were retrospective and had scarce forecasting capacity (Liu & Zhou, 2024). In addition, rainfall-based indices usually cannot measure stress on drought caused by temperature, especially with a warmer climate where evapotranspiration is the primary contributor to the depletion of soil moisture (Roux & Kunert, 2024). Computational techniques and machine learning (ML), deep learning (DL) models have become widely used in climate and drought research due to their progress (Subramaniam & Raju, 2022). Artificial neural networks, support vector machine, long short-term memory (LSTM), gated recurrent unit (GRU), and convolutional neural network (CNN) are examples of algorithms that have shown better performance in nonlinear climatic relationships modeling (Parasar & Moral, 2025). Non-stationary climate time series are however characterized by long-term persistence, multiple scales, and therefore constraints long-horizon forecasting using independent ML and DL models (Ougahi & Rowan, 2025). In order to address these shortcomings, new research has suggested hybrid modeling methods combining signal decomposition methods, i.e. wavelet transform, variants of empirical mode decomposition, seasonal-trend decomposition, with learning algorithms (Isler et al., 2025). Such hybrid methods have demonstrated greater predictive power in that they divide long-term trends and seasonal cycles and high-frequency variations before training a model (Shahriar & Choi, 2025). However, the majority of the current research is devoted to the accuracy of predictions and comparing the models, and little attention is paid to transforming the forecasts into practical climate risk information (Mishra et al., 2023). Simultaneously, geospatial analysis, which is based on satellites, has become an effective method to study the dynamic of land surface temperature (LST) and heat stress in space (Mansouri et al., 2022). The Landsat imagery has been scaled to multi-decadal analysis at large scale to express the warming trends, the hotspots of the heat, and land-use-climate interactions (Qiao & Zhang, 2025). These kinds of studies can give useful spatial context to drought susceptibility but they are in most cases done without predictive climate modeling (Birant & Ghasemkhani, 2025). Due to this, most of the assessments cannot attribute future temperature projections to known spatial patterns of heat stress, which constrain the utility of such projections in proactive drought management (Barzigar & Allahyari, 2025). Although there is still a lot of progress in AI-based climate prediction and the study of heat stress on satellites, there are still several major gaps. First, there are no combined frameworks that provide long-term forecasting of temperatures and spatiotemporal mapping of heat stress to aid in drought risk evaluation (Zellou & Moçayd, 2023). Second, current literature in Bangladesh is focused on rain-induced drought, which does not fully accurately reflect the increased prevalence of temperature-induced drought due to climate warming (Roux & Kunert, 2024). Third, there is a paucity of research studies that expressly relate historical drought experience and future climate forecasts to determine future agricultural risk areas (Biazar & Golmohammadi, 2025). Lastly, there is a lack of data regarding the application of more sophisticated hybrid AI models in both data-limited and drought-prone areas like northwestern Bangladesh (Ayadi & Forouheshfar, 2025).

In order to fill these gaps, this research comes up with a hybrid model of artificial intelligence-geospatial framework that integrates the hybrid machine learning models of long-term temperature forecasting and the multi-decadal analysis of land surface temperature using satellites. The proposed study will focus on the Rajshahi district, and the goals are:

(i) assess the performance of advanced hybrid forecasting models combining signal decomposition and machine learning and deep learning models;

(ii) evaluate the warming patterns of the long-term and the rate of the high-temperature anomalies based on the predictions up to 2034;

(iii) examine spatiotemporal variations of surface heat stress on the data of Landsat-based LST from 1984 to 2024; and

(iv) discover drought risk and agricultural vulnerability zones due to temperature change through the spatial evidence to combine both the temporal and spatial measures.

The work will enhance the ability to predict droughts in the future and offer operational information on the effects of climate change on agriculture by connecting historical patterns of droughts, future temperature projections, and spatial heat stress dynamics to support the early warning of droughts and offer practical information on climate adaptation and sustainable agricultural planning. The suggested AI-GIS system is a scaled and transferable solution to climate-sensitive data-restrained areas, and will help to prevent drought hazards in Bangladesh as well as other drought-prone agrarian systems due to current climate change.

2. Study Area

The district of Rajshahi, as shown in Figure 1, is located in the northwestern part of Bangladesh, with a latitude of approximately 24.2-24.7°N and a longitude of 88.2-88.9°E. The district is located in the Barind Tract, which has comparatively low rainfall, high temperatures in summer, and soils that have low capability of retaining water, and is composed of clay. Indeed, the climate is characterized by a hot pre-monsoon, a concentrated monsoon, and a prolonged dry winter.

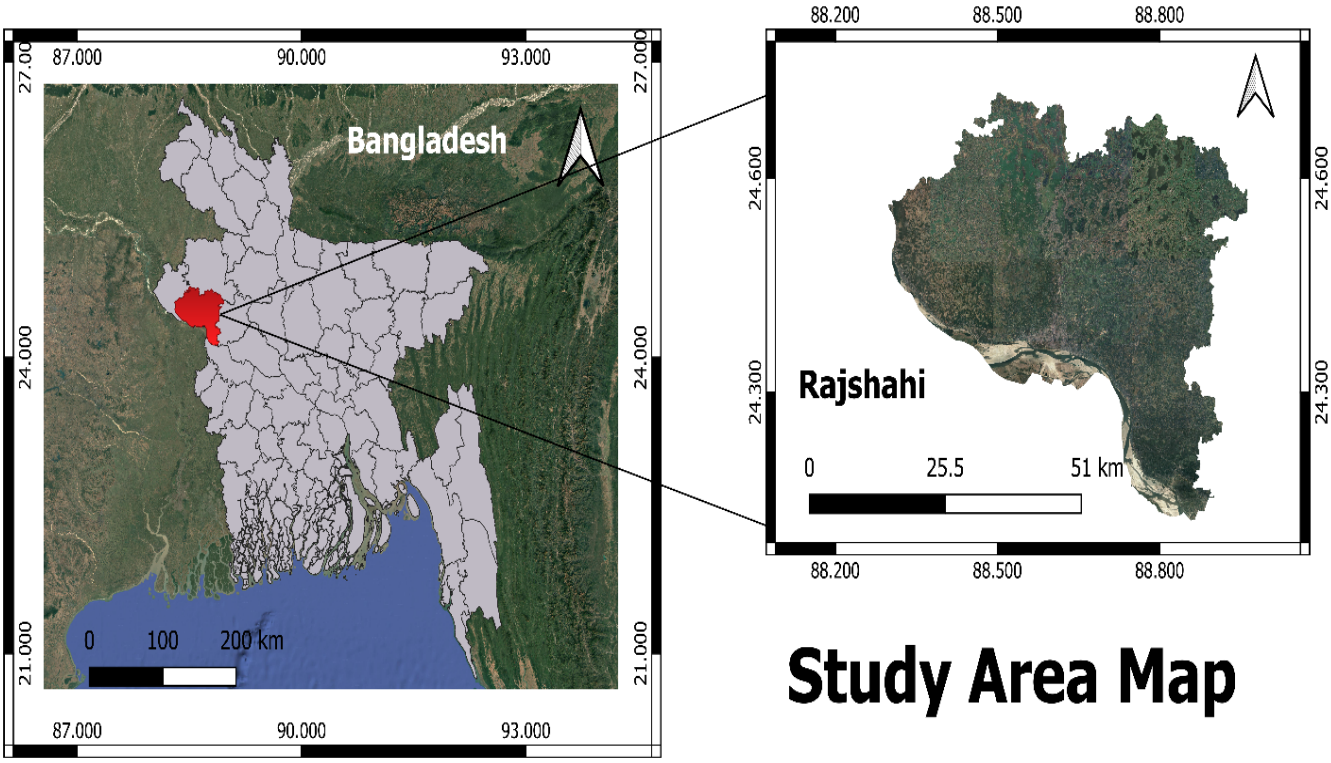

Fig.1 Study Area Map

Rajshahi has agriculture as the major source of livelihood, with the major crop types being Boro and Aman rice, wheat, pulses, and mango orchards. The area is also highly susceptible to climatic extremities that are driven by temperatures and has regular seasonal droughts, groundwater depletion, and irrigation pressure. These features make Rajshahi a perfect subject of study of integrated drought risk assessment through climate forecasting and spatial analysis.

3. Data Sources

3.1. Meteorological Data

The data on the mean temperature in Rajshahi on a monthly basis were received in the Bangladesh Meteorological Department (BMD) between 1980 and 2024. Quality checking of the data that was missing and consistency checking were done before the development of the model.

3.2 Satellite-Based Land Surface Temperature

The time period used was 1984 to 2024 to derive Landsat 5 TM, Landsat 7 ETM+, and Landsat 8 OLI/TIRS sensors of land surface temperature data. All satellite data were evaluated with the help of Google Earth Engine (GEE). Average LST maps were created on a period basis to analyze the spatial changes over a long period.

3.3 Ancillary Spatial Data

Administrative boundary shapefiles for the Rajshahi district were used for spatial masking and map visualization.

4. Methodology

This paper is based on an interdisciplinary artificial intelligence-geospatial model to estimate the long-term changes in temperature, drought threat, and agricultural exposure in Rajshahi district, Bangladesh. The workflow of the methodology comprises four primary elements: (i) data preprocessing, (ii) temperature forecasting, based on hybrid machine learning, (iii) spatiotemporal GIS analysis of the land surface temperature, and (iv) interpretation of drought and the risk of agricultural functions, driven by climate conditions.

4.1 Data Preprocessing

Data on monthly mean temperature available in the Bangladesh Meteorological Department (BMD) were initially taken through quality control interventions such as assessment of missing values and consistency tests. Because the time series of the climate was of a non-stationary and non-linear nature, there was no expectation of linearity or normality. This was done by data normalization before the models were trained to enhance numerical stability and performance.

4.2 Hybrid Machine Learning Framework for Temperature Forecasting

Ten hybrid models were created with the combination of signal decomposition methods and statistical and deep learning models to robustly capture long-term trends, seasonal variability, and extreme behavior of temperatures. The models were not separated, but divided into four methodological families, according to the learning philosophy and the climate signal representation in which they were developed. Such grouping is not redundant because it is methodologically clear.

4.2.1 Group 1: Signal Decomposition–Deep Learning Models

Models included:

- CEEMDAN–LMD–LSTM
- CEEMDAN–ELM–LSTM
- CEEMDAN–Informer–LSTM

This category combines Complete Ensemble Empirical Mode Decomposition with Adaptive Noise (CEEMDAN) and the state-of-the-art learning structures to tackle the nonlinear and non-stationary characteristics of the time series of temperature. CEEMDAN breaks down the original temperature series into intrinsic mode functions and a residual trend, and allows the distinction between long-term climatic trends and short-term variations. The decomposed features are then modeled with the help of Long Short-Term Memory (LSTM), Extreme Learning Machine (ELM), or Informer-based sequence models. The architectures have been especially useful in assembling temporal dependencies, long-range memory, and time-varying climate signals. This population is a blend of CEEMDAN and deep learners, which aims at capturing the consistent warming patterns and interannual variability with the local climate dynamics.

4.2.2 Group 2: Wavelet-Based Hybrid Models

Models included:

- Wavelet–CNN–LSTM
- Wavelet–VMD–LSTM
- Wavelet–ANFIS–SVR

Wavelet-based hybrids are used to represent a multi-scale representation of the temperature dynamics of time series; it is decomposed into time-frequency subcomponents. Wavelet transform allows the localized variations to be detected at various time scales, and this is especially applicable when the climate signals considered are seasonal cycle, inter-annual variation, or extreme events. Convolutional neural networks (CNN), LSTM networks, adaptive neuro-fuzzy inference systems (ANFIS), and support vector regression (SVR) are used to model the wavelet-decomposed signals in this category. These combinations enable the models to acquire hierarchical characteristics, nonlinear relations, and scale-dependent patterns. Wavelet-based hybrids are hence suitable for detecting sudden changes in temperature and the change in behaviour of the climate.

4.2.3 Group 3: Statistical–Deep Learning Hybrid Models

Models included:

- STL–ARIMA–BiLSTM
- SG–CEEMDAN–ARIMA–LSTM
- CEEMDAN–SARIMA–CNN

This category is a combination of classical statistical time-series models with deep learning architectures to utilize deterministic seasonal patterns and nonlinear patterns of residuals. Trend and seasonal components are separated by using seasonal and Trend decomposition based on the Loess (STL), Savitzky-Golay filtering (SG), and CEEMDAN. ARIMA and SARIMA series models can represent linear persistence and seasonal regularity, whereas deep learning BiLSTM, LSTM, and CNN can represent nonlinear residuals and complicated time interactions. This hybridization increases interpretability and forecasting precision, so this type of model is especially appropriate in climate time series that are highly seasonal and long-run persistent.

4.2.4 Group 4: Deep Sequence Learning Models

Model included:

- VMD–GRU–LSTM

This group is concerned with deep sequence learning for capturing the extremes of temperature and time. Variational Mode Decomposition (VMD). The VMD is initially used to separate the signal into frequency-limited modes of the temperature signal. In turn, these components are modeled with the help of gated recurrent unit (GRU) and LSTM networks to learn sequential dependencies and the behavior of extreme temperatures. VMD-GRU-LSTM is specifically effective to showing sharp change instances, anomalous warming instances, and long-term high-temperature episodes, and these are significant to drought early warnings and climate risk evaluation.

Table 1. Comparative summary of advanced hybrid decomposition–learning models for temperature forecasting, highlighting algorithmic structure, key hyperparameters, strengths, limitations, and representative application scenarios.

Model Name	Algorithm Type	Key Hyperparameters	Advantages	Limitations	Typical Use Case (Temperature Forecasting)
CEEMDAN-LMD-LSTM	Hybrid (CEEMDAN + LMD + LSTM)	CEEMDAN decomposition; LMD on high-frequency components; LSTM with 50 hidden units; Adam optimization; early stopping	Captures both high- and low-frequency components; robust temporal modeling with LSTM (Hochreiter & Schmidhuber, 1997; Kingma & Ba, 2014; Smith, 2005; Torres et al., 2011)	Computationally expensive due to multiple decompositions; requires careful parameter tuning.	Medium- to long-term forecasts where both high-frequency noise and long-term trends matter
Wavelet-VMD-LSTM	Hybrid (Wavelet + VMD + LSTM)	Wavelet decomposition (db4, level=3); VMD with K=4; LSTM per mode	Multi-resolution analysis with frequency mode separation; effective for nonstationary series (Daubechies, 1992; Dragomiretskiy & Zosso, 2014; Hochreiter & Schmidhuber, 1997)	Parameter selection for wavelets and VMD can be complex, with a high computational cost	Forecasting seasonal and cyclic temperature variations with noise reduction
SG-CEEMDAN-ARIMA-LSTM	Hybrid (Savitzky–Golay + CEEMDAN + SARIMA + LSTM)	SG filter: window=11, polynomial=3; CEEMDAN decomposition; SARIMA for linear IMFs; LSTM for nonlinear	Combines statistical (SARIMA) and deep learning for trend and residual modeling (Savitzky & Golay, 1964; Hyndman & Athanasopoulos, 2018; Hochreiter & Schmidhuber, 1997; Torres et al., 2011)	Model complexity: multiple stages require consistent preprocessing	Long-term trend forecasting with short-term variability in temperature data

STL-ARIMA-BiLSTM	Hybrid (STL + SARIMA + BiLSTM)	STL decomposition; SARIMA for trend; BiLSTM for residuals	Separates trend/seasonal/residual; BiLSTM captures bidirectional dependencies (Cleveland, 1990; Hyndman & Athanasopoulos, 2018; Schuster & Paliwal, 1997)	Seasonal extrapolation assumes periodicity; it may underperform on irregular patterns	Seasonal temperature forecasting with strong recurring patterns
CEEMDAN-Informer-LSTM	Hybrid (CEEMDAN + Informer + LSTM)	CEEMDAN decomposition; Informer for trends; LSTM for details	Informer handles long sequences efficiently; LSTM models high-frequency fluctuations (Torres et al., 2011; Zhou et al., 2021; Hochreiter & Schmidhuber, 1997)	Informer tuning complexity requires significant data for training	Long-horizon forecasting with mixed-frequency temperature variations
Wavelet-CNN-LSTM	Hybrid (Wavelet + CNN + LSTM)	Wavelet decomposition; CNN with 32/16 filters, kernel size=2; LSTM layers	CNN captures local patterns; LSTM models sequential dependencies (Daubechies, 1992; LeCun et al., 2015; Hochreiter & Schmidhuber, 1997)	Risk of overfitting with small datasets; sensitive to wavelet parameters	Short- to medium-term forecasts where spatial-like features in time series are present
VMD-GRU-LSTM	Hybrid (VMD + GRU + LSTM)	VMD with K=5; GRU (64 units); LSTM (32 units)	GRU reduces computation; LSTM refines temporal modeling (Dragomiretskiy & Zosso, 2014; Cho et al., 2014; Hochreiter & Schmidhuber, 1997)	Two-stage RNN architecture increases complexity; requires large data	Capturing mixed linear-nonlinear modes in medium-term temperature forecasts

CEEMDAN-SARIMA-CNN	Hybrid (CEEMDAN + SARIMA + CNN)	CEEMDAN decomposition; SARIMA for trends; CNN with 32 filters, kernel size=3 for details	Statistical modeling of trends with CNN extraction of complex residual features (Torres et al., 2011; Hyndman & Athanasopoulos, 2018; LeCun et al., 2015)	CNN may miss long-range dependencies; SARIMA assumes linearity in trends	Forecasting temperature with clear long-term trends and complex short-term variations
CEEMDAN-ELM-LSTM	Hybrid (CEEMDAN + ELM + LSTM)	CEEMDAN decomposition; ELM for linear IMFs; LSTM for nonlinear	ELM offers rapid training; LSTM handles nonlinear sequences (Torres et al., 2011; Huang et al., 2006; Hochreiter & Schmidhuber, 1997)	ELM may underfit complex linear trends; balancing ELM/LSTM output is tricky	Rapid temperature predictions where speed is critical
Wavelet-ANFIS-SVR	Hybrid (Wavelet + SVR replacing ANFIS)	Wavelet decomposition; SVR with RBF kernels	Robust regression for nonlinear temporal patterns; avoids ANFIS complexity (Daubechies, 1992; Vapnik, 1995; Jang, 1993)	SVR kernel/parameter tuning needed; no explicit trend-seasonal separation	Temperature forecasting with nonlinear dynamics and noise

4.3 Spatiotemporal GIS analysis: Land Surface Temperature.

The land surface temperature (LST) data of Landsat sensors were accessed from satellites to analyze the long-term spatial dynamics of heat in the Rajshahi district based on Google Earth Engine. To locate the tendencies of warming, the development of thermal hotspots, and a spatial heterogeneity in surface temperature, period-wise average LST maps (1984-2024) were created.

4.4 Agricultural Risk Interpretation and Drought.

Observed patterns of LSTs were then interpreted together with the forecasted patterns of temperature to determine the risk of drought and agricultural vulnerability. High and consistent temperatures were associated with high demand for evapotranspiration, loss of soil moisture, and possible crop stress. The novel combination of the interpretation offers a climate-informed foundation of drought early warning and agricultural adaptation planning.

4.5 Evaluation Matrices

The results of the models in terms of temperature prediction were studied by the application of various evaluation indicators. These measures were used on 10 hybrid models to allow a fully assessed evaluation of the accuracy and reliability of the prediction of these models. The matrices that are used are the following:

- **Mean Absolute Error (MAE)**

In MAE, the difference between the projected and the actual values is calculated, with each error being considered equally.

$$MAE = \frac{1}{N}\sum_{i=1}^{N} |y_i - \hat{y}_i| \dots \dots \dots (1)$$

MAE is more precise than other matrix techniques. This is a sure way by which prediction error can be more accurately measured.

- **Root Mean Squared Error (RMSE)**

Root Mean Squared Error (RMSE), which is easy to interpret and gives data about the mean errors in prediction, is based on the square root of Mean Squared Error (MSE).

$$RMSE = \sqrt{MSE} = \sqrt{\frac{1}{N}\sum_{i=1}^{N} (y_i - \hat{y}_i)^2} \dots \dots \dots (2)$$

It is useful in time series prediction since one can trace the variation of errors and reduce errors; the smaller the number, the more accurate the model is.

- **Coefficient of Determination (R^2 Score)**

Assessment of the predictive power of independent variables can be done with the R2 score. The proportion of the volatility of the actual data that the model is able to predict. When the values range between 1 and 0, the perfect prediction will be presented; otherwise, the variability of the data will be addressed.

$$R^2 = 1 - \frac{\sum_{i=1}^{N} (y_i - \hat{y}_i)^2}{\sum_{i=1}^{N} (y_i - \bar{y}_i)^2} \dots \dots \dots (3)$$

Improved functionality of the model. The dataset was closely monitored and used to model, especially in climatic data, based on the increased R2 values.

- **Mean Squared Error (MSE)**

MSE is a regression model of loss functions that is widely used in estimating the square of average errors to provide results between actual and expected performance.

$$MSE = \frac{1}{N}\sum_{i=1}^{N} (y_i - \hat{y}_i)^2 \dots \dots \dots (4)$$

Where N = total number of observations (y (i) = the actual temperature value at time i and y i = the predicted temperature value at time i?

5. Results and Discussion

5.1 Performance Evaluation of Hybrid Models

All machine learning (ML), deep learning (DL), and hybrid models were tested on the predictive performance, which was measured in terms of MAE, RMSE, MSE, and coefficient of determination (R^2). The assessment was done on the testing sample to determine the ability to generalize and the strength. The results are explained in the context of methodological consistency and reliability between model groups, instead of the individual model supremacy, which is more suitable in climate and drought-related studies.

5.1.1 Group-Wise Model Performance Comparison

1. **Group 1: Signal Decomposition–Deep Learning Models**

This category of models uses Complete Ensemble Empirical Mode Decomposition with Adaptive Noise (CEEMDAN) with the latest deep learning networks to efficiently model nonlinear, non-stationary, and multi-scale properties of temperature time series. On the whole, these models demonstrated high levels of predictive performance on all measures of evaluation, where the MAE and RMSE values are consistently lower, and the scores of R^2 are higher than those of non-decomposed or purely statistical methods. The improved performance can be attributed to the capability of CEEMDAN to separate intrinsic oscillatory and long-term trends before the prediction by deep learning.

- **CEEMDAN–LMD–LSTM**

The CEEMANLMDLSTM model is a hybrid of CEEMDAN-based signal decomposition, Local Mean Decomposition (LMD), and LSTM learning to address both long-term climatic variations and short-term variability.

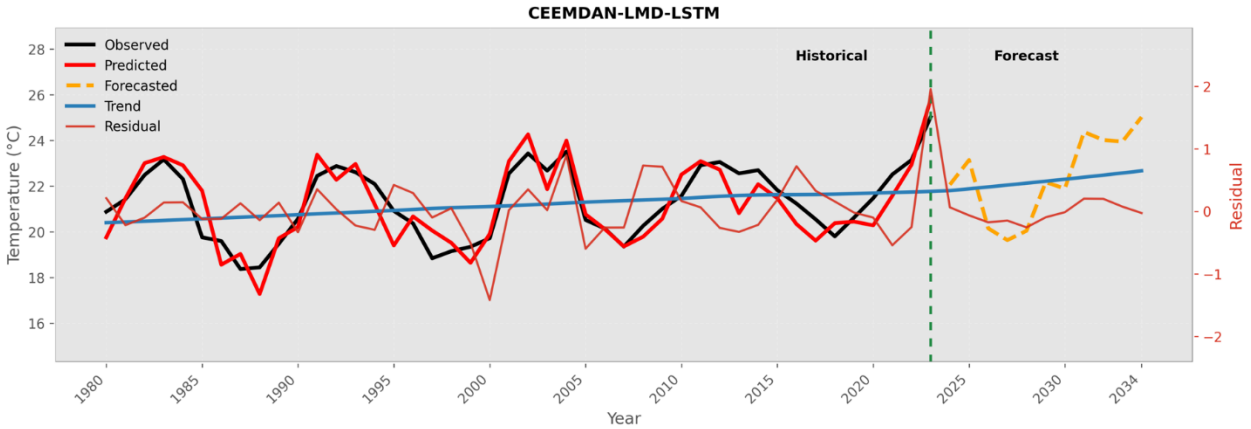

Fig. 2. Comparison between observed and predicted monthly temperature series using CEEMDAN–LMD–LSTM

As shown in Figure 2, the forecasted series of temperature is quite close to the observed values, especially in the trending seasonal cycles and slow warming tendencies. The small deviations are mainly found in sudden changes in temperature, which means that the model has the ability to average noise and still retain significant climate information. The dispersion of the errors illustrated in the figure is relatively low, which supports the strength of using such a hybrid framework to model temperature persistence when used to assess droughts.

- **CEEMDAN–ELM–LSTM**

CEEMDANELM LSTM architecture merges CEEMDAN and Extreme Learning Machine (ELM) along with the LSTM architecture to improve the efficiency of learning and, at the same time, ensure that temporal dependencies in the dataset are preserved.

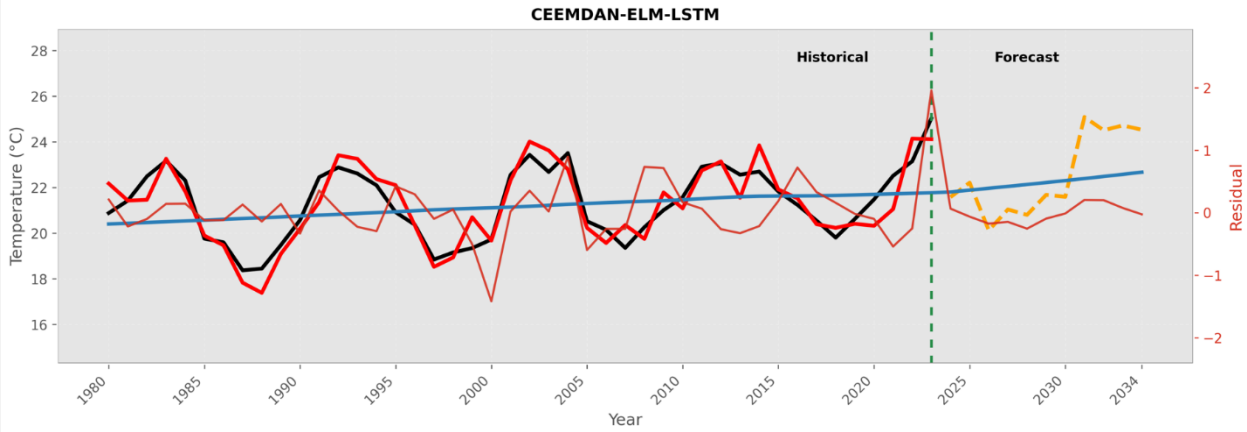

Fig. 3. Comparison between observed and predicted monthly temperature series using CEEMDAN–ELM–LSTM

This model, as indicated in Figure 3, illustrates high similarity in the observed and predicted temperatures with less phase lag between CEEMDAN and CEEMDAN-LMD-LSTM and high responsiveness to short-term dynamics. This capability of the model to quickly adjust to the changing temperature patterns is indicative of the performance of ELM in capturing the nonlinear residual elements, whereas the layer of the LSTM provides continuity of the long-term patterns of climate.

- **CEEMDAN–Informer–LSTM**

Of the Group 1 models, CEEMDAN -Informer -LSTM had the best overall predictive accuracy. This model uses the effectiveness of the Informer architecture in modelling long-term temporal relationships efficiently, which makes it especially effective in long-term climate projections.

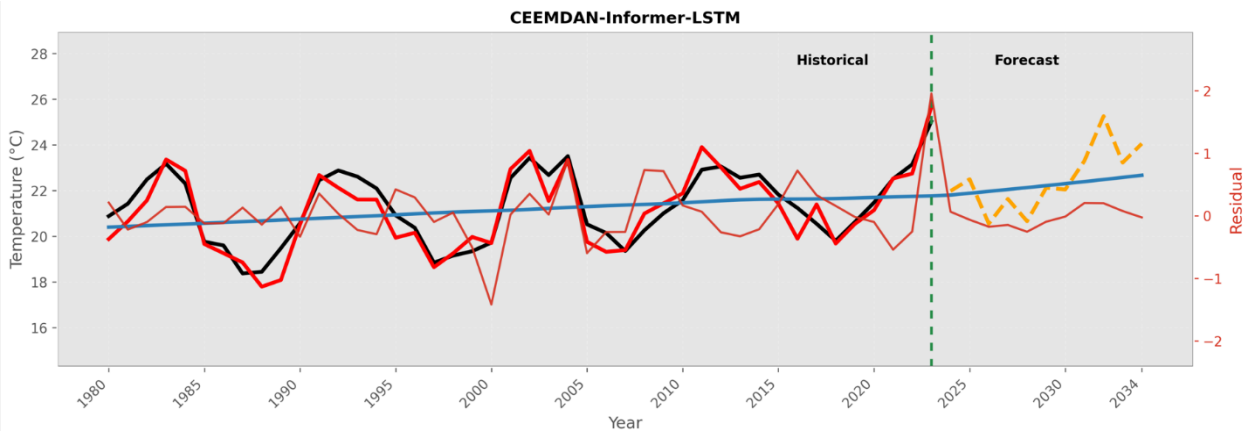

Fig. 4. Comparison between observed and predicted monthly temperature series using CEEMDAN–Informer–LSTM

As can be seen in Figure 4, the series of predicted temperatures not only concur with the actual temperatures but also maintain a continuity of trend over the long run and interannual variability with very little smoothing bias. The smaller amplitude distortion and the narrow gap in the confidence show enhanced learning in both persistent warming signals and temporal memory.

The compensation of low error dispersion and consistent reproduction of the trend in the figure supports the effectiveness of the CEEMDAN, with the addition of attention-driven deep-learning frameworks. This is essential to climate impact research, in which a sound model of long-term warming paths is necessary to produce information on drought risks, as this is directly dependent on the representation.

- **Group-Level Interpretation**

Together, the numbers indicate that the decomposition using CEEMDAN can be applied to deep learning to provide a significant boost to its performance by alleviating noise, isolating physically meaningful temperature factors, and stabilizing the performance of the forecast. The overlapping of the predicted and observed series by all three models is a sign that the warming signal that is being observed in Rajshahi is not model-specific but rather solid. These are what make Group 1 models especially applicable in downstream climate risk analytical applications and/or early-warning drought applications.

2. Group 2: Wavelet-Based Hybrid Models

Hybrid models Wavelet-based hybrid models combine an architecture based on time-frequency signal decomposition with machine learning and deep learning models to encode multi-scale variations in the temperature in the signal. These models showed competitive behavior in all the evaluation measures, especially in capturing seasonal variability, transitional climate behavior, and short-term fluctuation within long-run warming trends.

- **Wavelet–CNN–LSTM**

Wavelet-CNN-LSTM is an algorithm that uses a combination of wavelet transform, convolutional, and recurrent neural networks to extract a hierarchical temporal signal from the decomposed temperature signal.

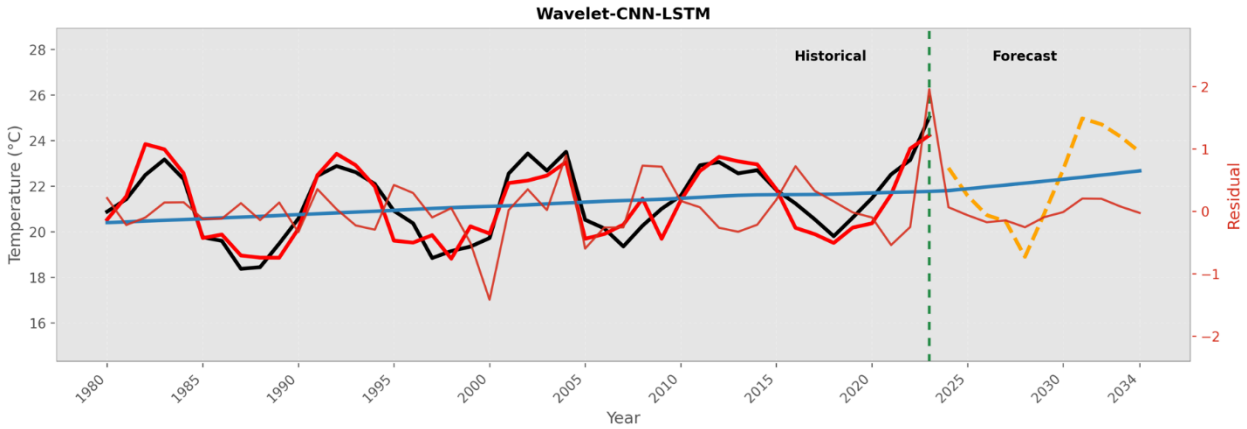

Fig. 5. Observed versus predicted temperature series produced by Wavelet–CNN–LSTM

As shown in Figure 5, the predicted temperature series is very similar to observed seasonal oscillations with good representations of periodic warming and cooling on-cycles. Convolutional layers are used to improve the extraction of features by the wavelet sub-bands, whereas the LSTM component maintains time continuity. The fact that, on sudden transition, there are minor deviations, is an indication that the model is sensitive to high-frequency variability; however, overall consistency proves the appropriateness of the model in the description of transitional climate behavior.

- **Wavelet–VMD–LSTM**

The Wavelet VMD LSTM model is the combination of wavelet decomposition, variational mode decomposition (VMD), and the learning process of the long-term short-term memory (LSTM) neural network, which enhances the

representation of low- and high-frequency temperature variations. This model has the highest level of agreement between measured and predicted temperatures of Group 2 models,

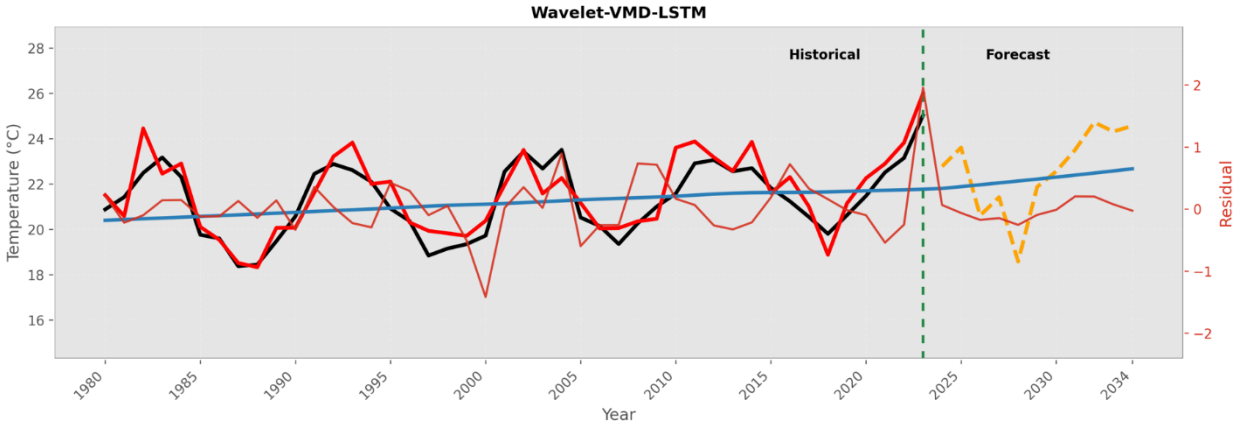

Fig. 6. Observed versus predicted temperature series produced by Wavelet–VMD–LSTM

as illustrated in Figure 6. The long-term trends of the predicted series are well maintained, and on the other hand, the short-term fluctuations are well captured with little noise. The increased values of R^2 and decreased values of MSE of this model suggest that it is able to learn better the intrinsic temperature modes, which is the main strength of this model in the modeling of non-stationary climate signals.

- **Wavelet–ANFIS–SVR**

The Wavelet-ANFIS-SVR model is a combination of wavelet-based decomposition, adaptive neuro-fuzzy inference, and support vector regression to gain the nonlinear dependence of temperature data. The general seasonal patterns and long-term trends are replicated by the model

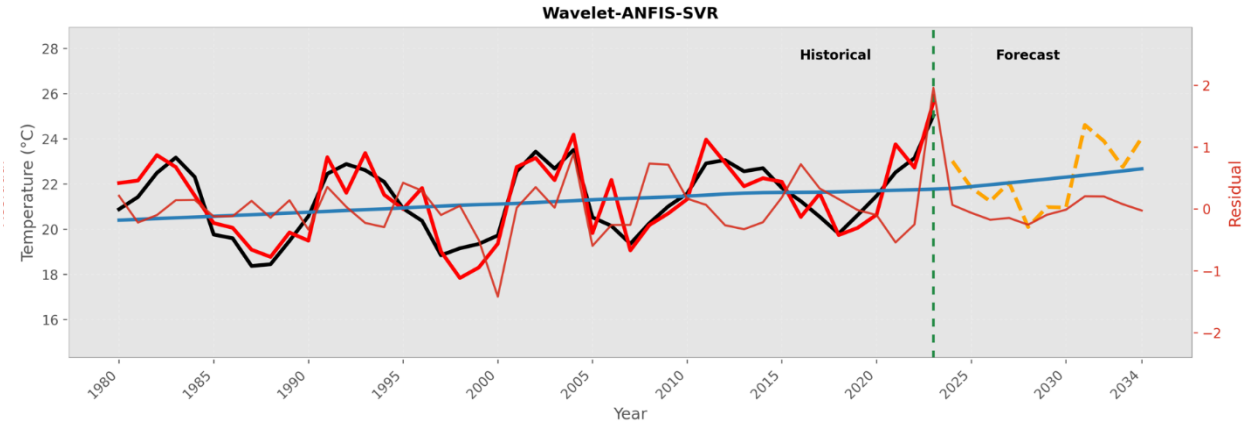

Fig. 7. Observed versus predicted temperature series produced by Wavelet–ANFIS–SVR

As shown in Figure 7, there is a slight smoothing, which can be seen in extreme temperature peaks. This is an indication that the model is strong in generalization and interpretability, though with a relative lack of sensitivity to sudden changes in temperature extremes. However, the general similarity between observed and predicted values supports the fact that neuro-fuzzy learning is effective in the representation of climate time series.

- **Group-Level Interpretation**

By combination, the hybrid models based on the wavelet have shown great ability of capturing the multi-scale dynamics of temperature, especially seasonal variability and intermediate-frequency climate signals. The excellent performance of the Wavelet-VMD-LSTM indicates that the integration of the wavelet and variational mode decomposition can be beneficial in improving signal separation and reducing the mode mixing. The fact that the three models converge indicates that wavelet-based decomposition is a reliable and consistent basis to modeling non-stationary behavior of temperature, thus these models can be used in the evaluation of variability of climates, and in drought-type applications.

3. Group 3: Statistical–Deep Learning Hybrid Models

The hybrid models of statistical-deep learning combine classical time-series models with the deep learning models to learn both linear seasonal persistence and nonlinear residual dynamics. These models also demonstrated predictive stability in terms of evaluation measures, with moderate values of MAE and RMSE, and consistent R^2 scores, indicating their effectiveness in modeling autoregressive behavior and seasonal climatic patterns.

- **STL–ARIMA–BiLSTM**

STL-ARIMA-BiLSTM is a model that can be used to model the seasonal and trend of deterministic components with the help of Loess (STL) and ARIMA modeling and bi-directional LSTM learning to model nonlinear temporal interactions. The predicted temperature series

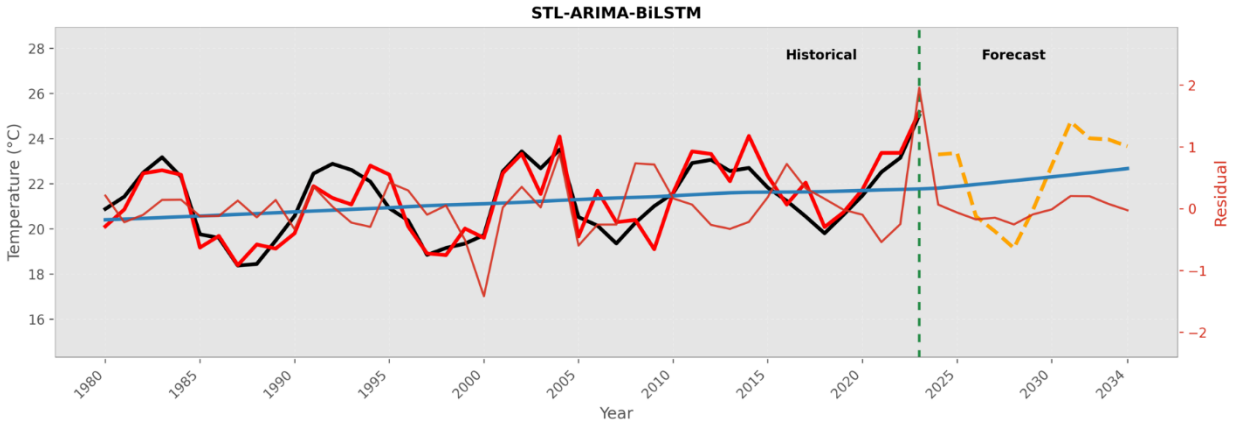

Fig.8. Comparison of observed and predicted temperature values using STL–ARIMA–BiLSTM

As shown in Figure 8, it remarkably follows the observed seasonal cycles, and the periodic warming and cooling cycles are effectively represented. The bidirectional LSTM element enhances the temporal context sensitivity through learning the forward and backward dependencies that lead to the continuity of trend stability. The slight underestimation during sharp temperature peaks implies that there was a conservative reaction to extreme variability which is a factor that helps the model to be overall stable.

- **SG–CEEMDAN–ARIMA–LSTM**

The SG-CEEMDAN-ARIMA-LSTM model combines Savitzky-Golay (SG) filtering as well as CEEMDAN-based decomposition with ARIMA and LSTM learning with the aim of improving signal smoothness and nonlinear residual modelling.

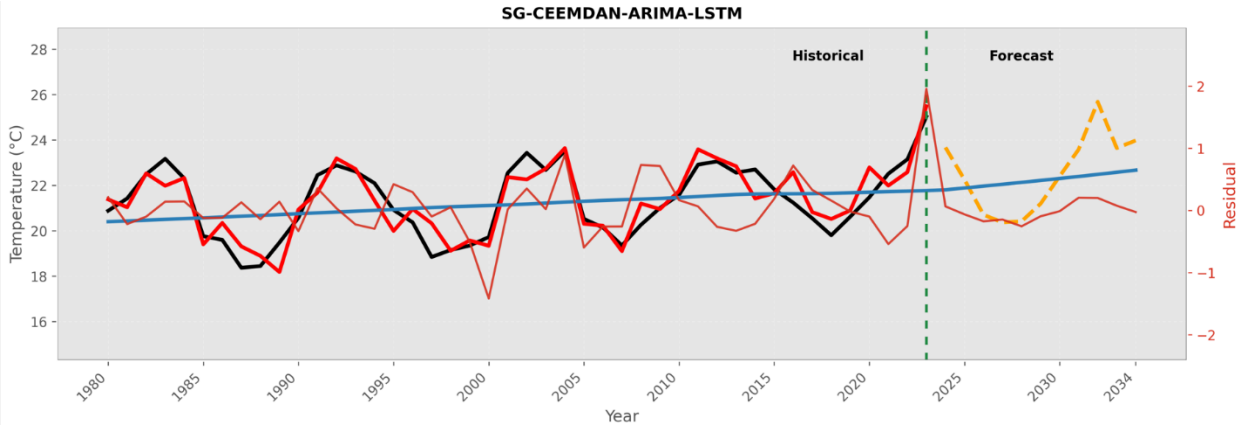

Fig.9. Comparison of observed and predicted temperature values using SG–CEEMDAN–ARIMA–LSTM

According to Figure 9, this model shows better correlation of observed and predicted temperatures than other Group 3 models. The series below, which is the predicted series, is doing a great job in capturing seasonal persistence and gradual warming trends, and it incurs lower phase lag, as well as a better responsiveness to transitional variation. The comparatively large R^2 and smaller error dispersion of this model indicate the advantage of the model in integrating statistical seasonality modeling with residual correction through deep learning.

- **CEEMDAN–SARIMA–CNN**

The CEEMDAN-SARIMA-CNN model incorporates CEEMDAN decomposition with Seasonal ARIMA (SARIMA) and convolutional neural networks to detect both the linear and nonlinear localized patterns of seasonality. With the general seasonal behaviour and long-term trends being reproduced

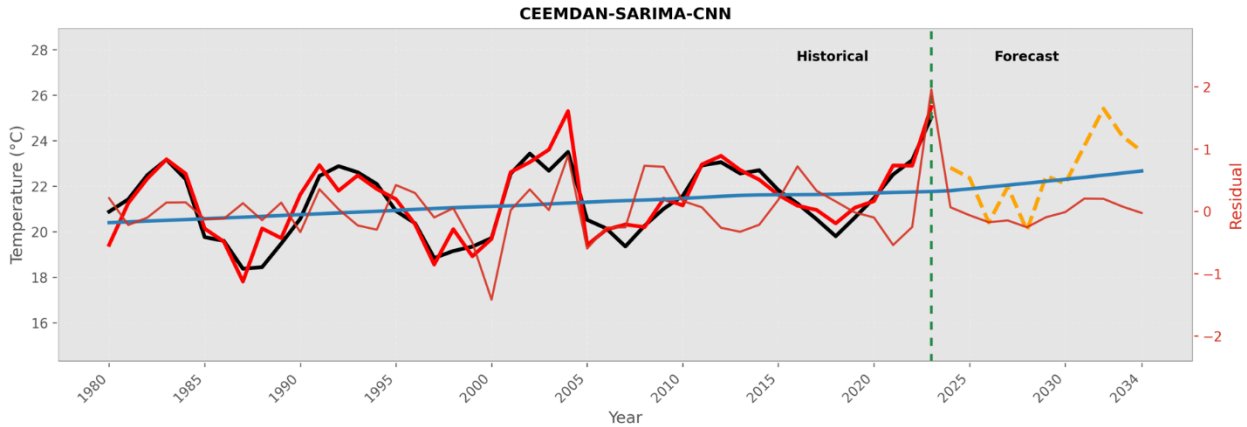

Fig.10. Comparison of observed and predicted temperature values using CEEMDAN–SARIMA–CNN

As shown in Figure 10, slight smoothing is observed in the high-amplitude temperature swings of the model. The CNN element improves the extraction of features of decomposed signals, whereas the SARIMA structure preserves seasonality. This equilibrium helps in improving interpretability and the strength of this model, although with a minor diminished sensitivity to extreme temperature incidences.

- **Group-Level Interpretation**

On the whole, statistical-deep hybrid models show good performance in modeling seasonal persistence and autoregressive climate behavior that are inherent attributes of temperature time series. The better performance of SGCEERAARIMALSTM highlights the importance of the combination of statistical decomposition with the learning

of non-linear residual to enhance predictive performance. Even though these models are slightly inaccurate compared to purer, deeply hybrid models, they are more useful in climate studies where transparency and consistency are vital.

4. Group 4: Deep Sequence Learning Models

Deep sequence models of learning are based on learning long-term temporal dependencies, as well as extreme behavior of climate time series, with recurrent neural network models. In the paper, the VMDGRU-LSTM model is the representative of this methodology family and is developed to improve the learning of persistent warming signals and anomalous temperature incidences applicable to drought risk assessment.

- **VMD–GRU–LSTM**

VMD-GRU-LSTM is a combination of Variational Mode Decomposition (VMD) with a gated recurrent unit (GRU) network and long short-term memory (LSTM) network, which can be used to efficiently model a complicated temporal relationship in temperature records. VMD breaks down the temperature series of origin into frequency-limited intrinsic modes, which minimizes mode mixing and allows major temperature signals to be separated more clearly. These disintegrated parts are then successively trained through GRU and LSTM structures to embrace both the short-term variability as well as long-term memory impacts.

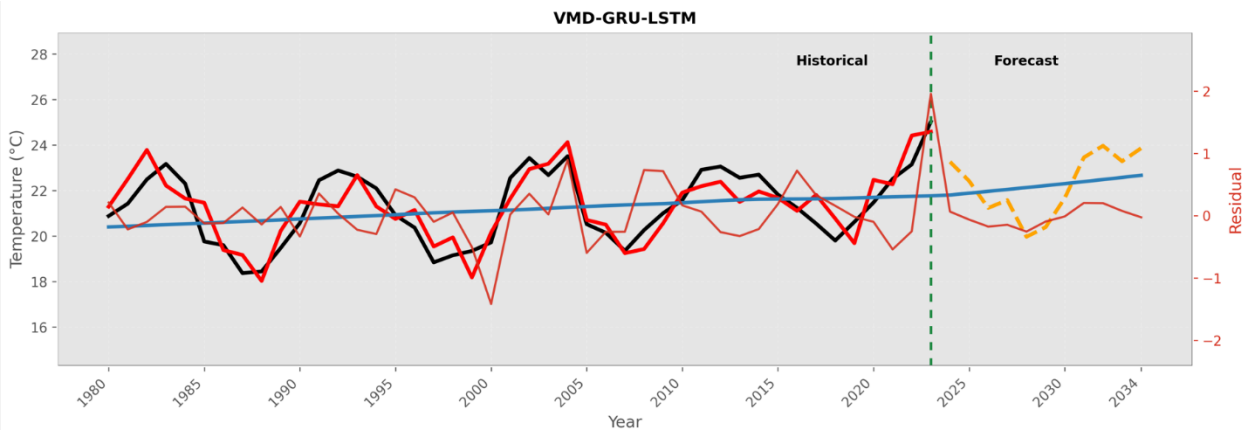

Fig.11. Observed and predicted temperature series generated by the VMD–GRU–LSTM model.

As shown in Figure 11, the modeled temperature sequence shows a high level of correlation with the real numbers over the entire duration of the study, especially in long warming intervals and temperature extreme events. The model is also effective in maintaining the intensity and timing of extreme temperatures, which exhibits less phase lag, and reproducible fixed trends. The small variations in RMSE and the comparatively high values of R^2 depict good predictive power and good explanatory power, particularly when it comes to the representation of continuous thermal stress conditions.

The capability of the VMD-GRU-LSTM model to store the temporal memory and extreme behavior of the model makes it especially applicable to climate applications where prolonged heat exposure becomes a major contributor to the formation of drought and plant stress. In spite of the fact that this model does not perform better than decomposition deep hybrid frameworks in the overall accuracy, it is stronger in modeling extreme and sustained temperature fluctuations with a high level of temporal coherence.

5.2 Long-Term Temperature Forecasting

Decades-long temperature predictions based on the most effective hybrid projections indicate that there is a consistent and coherent warming pattern in the district of Rajshahi through to the 2030s. According to Figure 12, the hybrid structures always indicate an upward curve in the temperature distributions with the passing of successive decades,

which means that there is a systematic increase in central tendency as well as the upper ends. In Figure 12, the decadal boxplot analysis provides a view of the graphic representation of the temperature features that have been associated with time. Median temperatures are relatively lower, and the interquartile ranges are also smaller in the past decades (1980-1999), and hence the thermal conditions were not very extreme. Conversely, however, recent decades (2000-2024) report an evident movement towards higher median values with broader distributions, which means temperature variability and the overall growth in the proportion of warm anomalies.

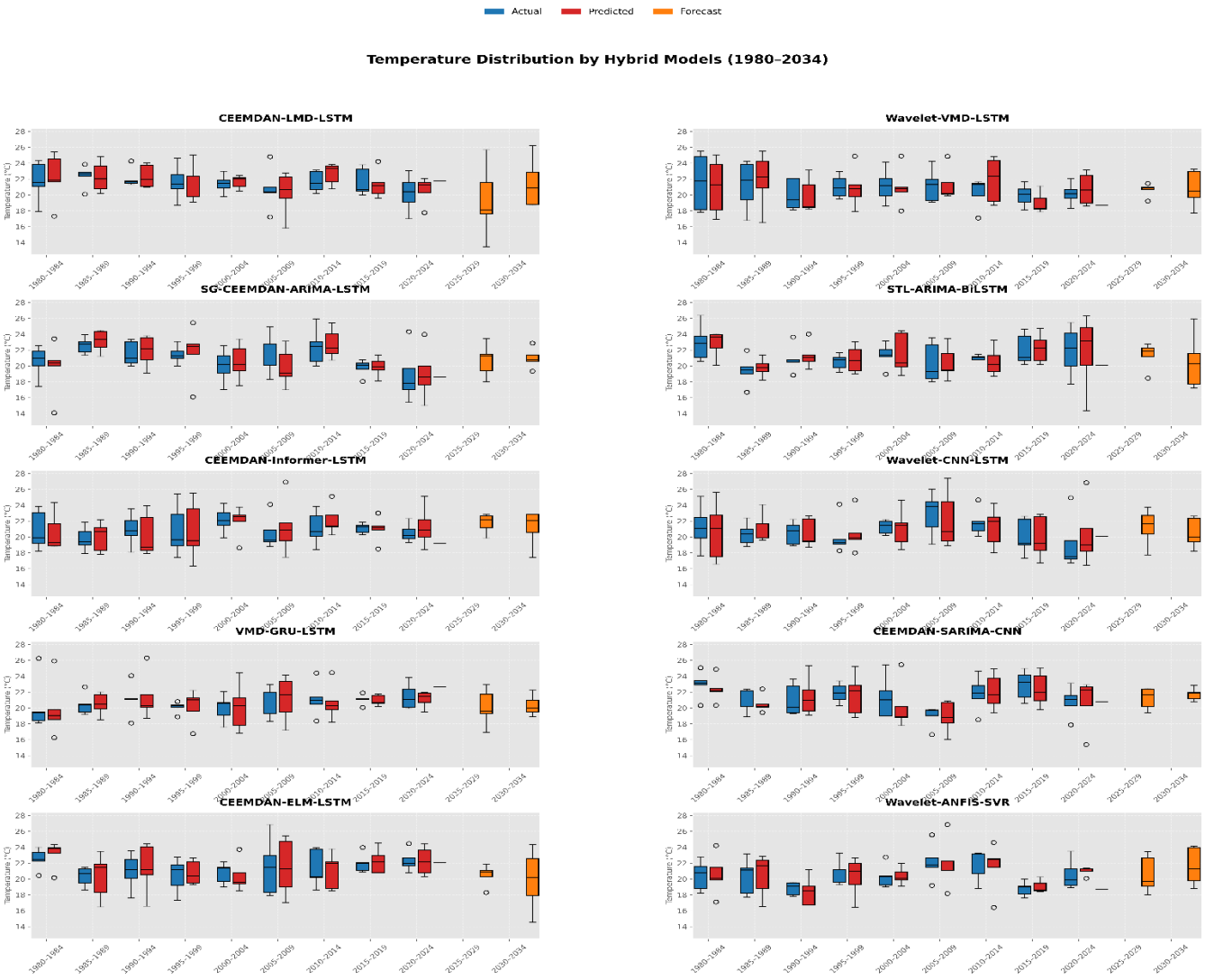

Fig.12. Decadal temperature distribution and long-term forecasting using hybrid models

This warming signal is further enhanced by the forecasted periods (2025-2029 and 2030-2034), which are represented by the orange boxplots in Figure 12. These forecasts project high median temperatures and larger upper percentiles in all the hybrid models, implying a greater tendency to experience high temperature durations. The uniformly raised upper whiskers through models indicate the rising frequency and intensity of extreme heat events and not the cases of isolated outliers. Notably, the convergence of temperature distributions of these multiple families of methods, signal decomposition, deep learning, wavelet-based hybrids, statistical deep hybrids, and deep sequence learning, shows that there is a good convergence in the long-term project of warming. This inter-model consistency minimizes uncertainty that might be involved when a particular model is used and makes people very confident about the stability of the trends of the projected temperatures. The mechanisms of the observed increase in the upper temperature distributions have serious climatic consequences, with high temperatures being strongly associated with the heightened need for

evapotranspiration and the lack of moisture on the surface. As a result, the predicted warming pattern offers an essential basis to understand the future drought hazard and agricultural burden of Rajshahi district, accentuating the worth of hybrid AI-based forecasting in gauging climate effects instead of a strictly predictive comparison.

5.3 Quantitative Evaluation of Model Performance

The performance of all the hybrid models in terms of quantitative metrics was assessed, including MAE, MSE, RMSE, and coefficient of determination (R^2), as summarized in Table 2. These metrics measure the accuracy of prediction, sensitivity to large error variations, and explainability of temperature variability. By comparing models of advanced signal decomposition methods with deep learning architectures, it is found that in most cases, models that combine these two approaches had lower error levels and increased explanatory power, as demonstrated in Table 2.

Table 2. Quantitative Evaluation of Model Performance

Model	MAE	MSE	RMSE	R^2
CEEMDAN-LSTM	0.6882	0.9712	0.9855	0.6523
Wavelet-VMD-LSTM	0.0869	0.0126	0.1122	0.9885
SG-CEEMDAN-ARIMA-LSTM	2.2939	8.8402	2.9732	0.6807
STL-ARIMA-BiLSTM	0.3086	0.1288	0.3589	0.9953
CEEMDAN-Informer-LSTM	4.3806	26.1424	5.113	0.0558
Wavelet-CNN-LSTM	0.0374	0.0023	0.0483	0.9688
VMD-GRU-LSTM	0.3473	0.2073	0.4553	0.9903
CEEMDAN-SARIMA-CNN	0.0972	0.0127	0.1128	0.9999
CEEMDAN-ELM-LSTM	0.7844	1.0549	1.0271	0.954
Wavelet-ANFIS-SVR	2.5793	11.5673	3.4011	0.9311

The Wavelet-CNN-LST model had the lowest MAE (0.0374) and RMSE (0.0483), indicating that the accuracy of short-term predictions is high and the deviation observed between the model and the observed temperatures is minimal. Likewise, the values of MAE (0.0869) and RMSE (0.1122) for Wavelet-VMD-LSTM were minimal, with a high R^2 value (0.9885), which indicates an excellent ability to adhere to both seasonal and multi-scale variations in temperature. The CEEMDAN-SARIMA-CNN model had the highest R^2 value (0.9999) and the lowest MAE (0.0972) and RMSE (0.1128) values, which indicates that it has the best capacity to account for the variance in temperature observed. This demonstrates the effectiveness of combining CEEMDAN-based decomposition with statistical seasonality modeling and convolutional feature extraction, particularly in capturing structured climatic patterns. The statistical-deep hybrid models (E.g., STL-ARIMA-BiLSTM) also demonstrated good explanatory power (R^2 = 0.9953) with moderate error values, indicating that these models well represented seasonal persistence and autoregressive patterns. By contrast, SG-CEEMDAN-ARIMA-LSTM demonstrated relatively greater values of MAE and RMSE, implying a lesser sensitivity to short-term changes, but with a sufficiently high value of explanatory power.

The VMD-GRU-LSTM model exhibits a high R^2 value (0.9903) and a moderate RMSE value (0.4553), indicating strong capabilities in storing long-term temporal memory and maintaining long-term persistence of warming, making it particularly suitable to drought-related climate analysis. On the other hand, CEEMDAN-Informer-LSTM exhibited comparatively high error values and a low R^2 value, suggesting that it has limited explanatory power in the current data. This tendency can be explained by the fact that the Informer architecture relies on large-scale sequence learning, which may be less efficient when dealing with moderate-length climate time series that exhibit substantial seasonal structure.

The findings in Table 2 indicate that no single model prevails in all the assessment measures. Instead, their most reliable performance is modeled by those who have managed to balance well the noise reduction of decomposing models and the temporal representation of deep learning frameworks. The overlap of robust outcomes among several different hybrid frameworks strengthens the belief in the strength of the demonstrated warming trends. It allows us to use them to interpret the climate impacts instead of trying to optimize them with the help of algorithms.

5.3 Spatiotemporal Patterns of Land Surface Temperature

Landsat-derived multi-temporal land surface temperature (LST) maps give detailed information on the spatial development of the surface warming throughout the Rajshahi district over the past 40 years (Figure 13-22). Each of the panels depicts a four-year average LST distribution, which allows a uniform comparison over time of the thermal patterns.

- **Surface Temperature Distribution (1984–1987)**

The surface temperature of the land surface during 1984-1987 shows that mostly the thermal conditions in the Rajshahi district are cool to moderate. The interior and northern part is dominated by lower surface temperatures, which are defined by blue to cyan colors, and this implies that the land surfaces were relatively stable and thermally regulated at a relatively early time of observation. The areas of increased surface temperature are mostly restricted to areas of large river channels and the southwestern boundary areas. These warmer regions are shown in yellow to red color, indicating the areas of exposure like riverbanks, sand bars, and other low vegetation surfaces, where the local moisture content and sunlight exposure add to the localized accumulation of heat. Nonetheless, these hot spots are spatially alienated and disconnected.

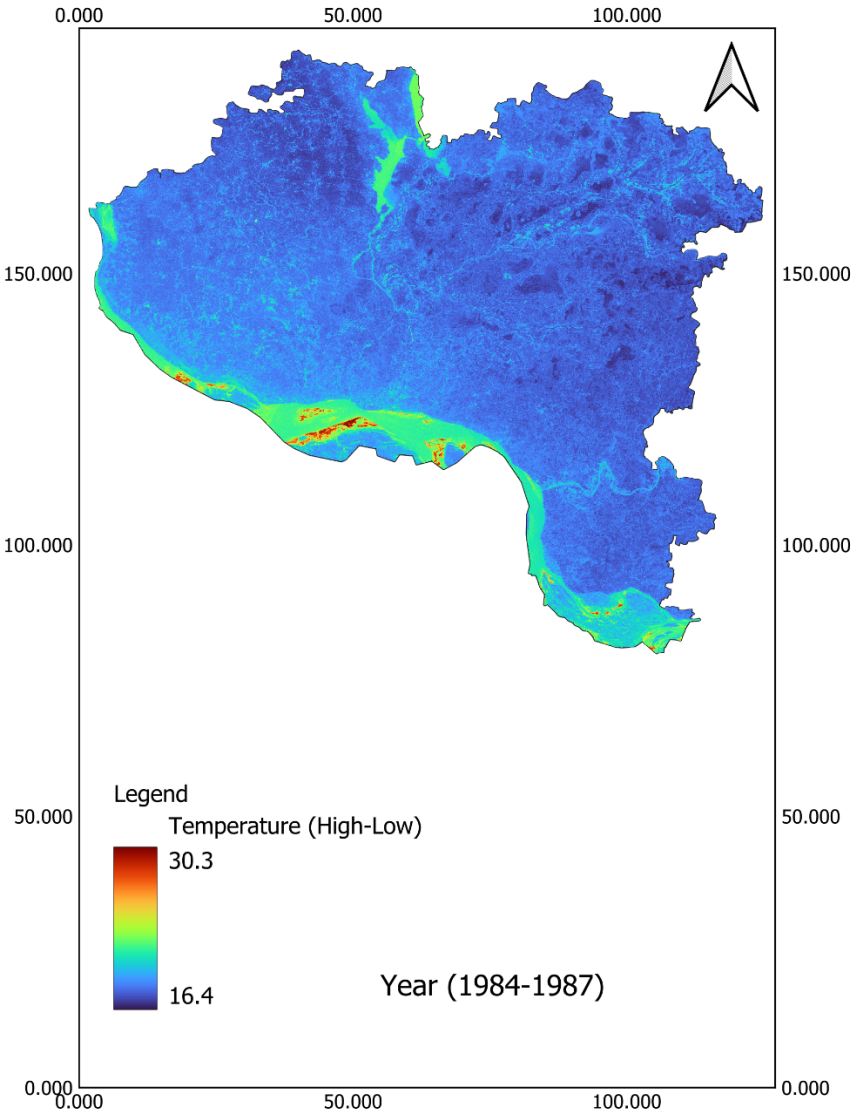

Fig.13. Spatiotemporal evolution of LST in Rajshahi district (1984–1987)

Moderate temperatures and low levels of spatial variation characterize the western and central agricultural landscape, which suggests a relatively equal relationship between land cover, soil moisture, and the atmospheric conditions. It is also noticeable that there are cooler patches around water bodies and along the drainage networks, indicating the cooling effect of the surface water at this time. The space-based distribution, in general, indicates the existence of a thermally uniform topography with discrete areas of heat that are mainly due to geomorphological and hydrological effects and not extensive warming of the land surface. The lack of large high-temperature clusters means that local surface heating was not strong in the middle of the 1980s, and the results can serve as a thermal reference point to the following decades.

- **Surface Temperature Distribution (1988–1991)**

The temperature field of the land surface over 1988-1991 shows a significant rise in spatial heterogeneity in comparison with the previous time. Although much of the area of the Rajshahi district is still under the moderate temperature conditions, warmer surface conditions are more pronounced in space, especially in the central and eastern areas. The areas with a cooler temperature, which are represented by a darker blue color, are concentrated in the northern and western parts of the district. The relevant areas are probably more vegetation cover and less surface

exposure, which is involved in improved thermal control. However, the central and eastern areas are less green and yellow, pointing to the overall increase in average surface temperatures.

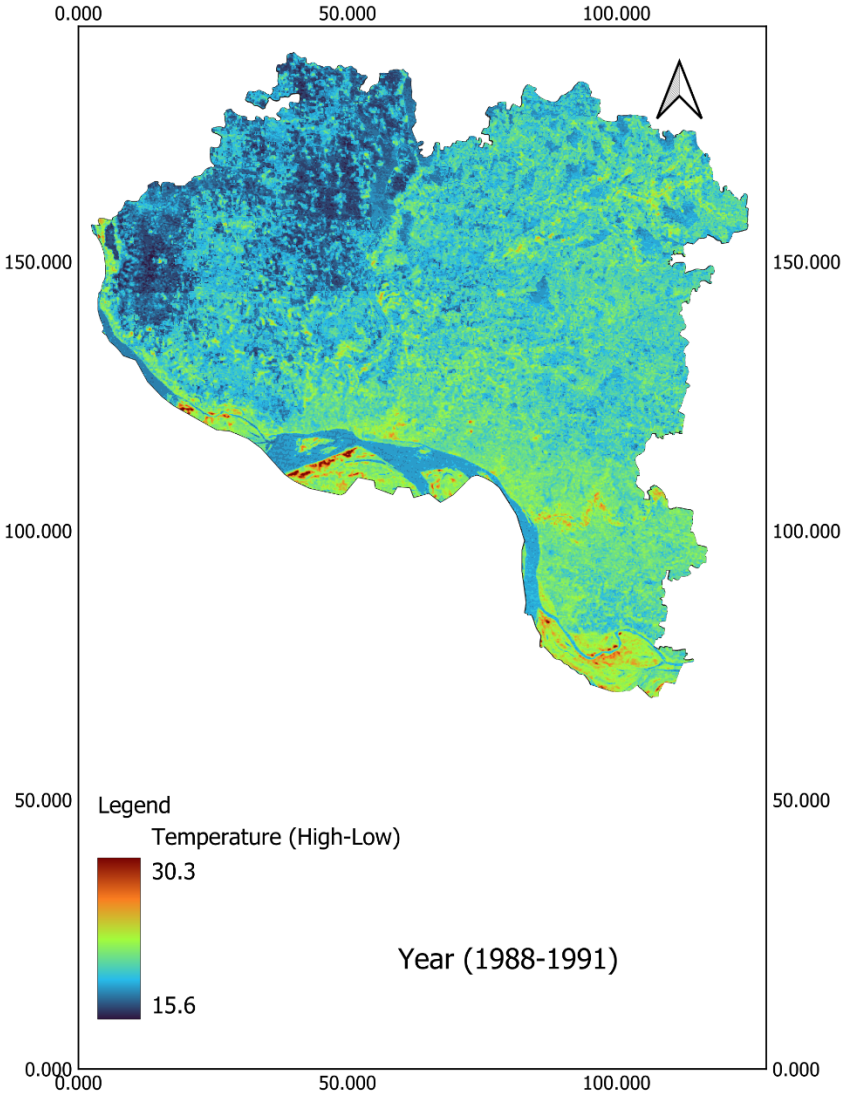

Fig.14. Spatiotemporal evolution of LST in Rajshahi district (1988–1991)

The areas of high temperatures are clearly observed along the major river corridors and the areas of the southern floodplain. These warmer linear patterns are indications of greater exposure of riverbanks and sandbars and neighboring cultivated lands with less moisture retention and surface perturbation of the land, raising the amount of heat. These hotspots are seen to be more continuous and extended in space as compared to the past decade. The southern and southeastern edges of the district are more strongly warmed with localized red and orange patches showing the anomalies of high temperature. This geomorphological increase of warm areas is indicative of the initial intensification of surface heating and not pure geomorphological influences. In general, the 1988-1991 interval is observed to be characterized by the shift of relatively homogenized thermal conditions to heterogeneous ones in terms of surface temperature patterns. The formation and growth of warmer areas are an indication of the beginning of organized warming of surfaces, which preconditions the appearance of more significant thermal heating in further decades.

- **Surface Temperature Distribution (1992–1995)**

The trend in land surface temperature distribution from 1992 to 1995 indicates that surface warming was more intense in the Rajshahi district than in past periods. Temperate to warm classes prevail in most areas of the landscape, as reflected by the prevalence of green and yellow hues in the central, western, and eastern areas. The zones of high temperatures are more spatially continuous and extensive, especially in the river corridors of the south and other floodplain areas located near them. The red and orange spots along these areas signify high surface heating, which is related to bare riverbanks, sandbanks, and highly cultivated lands. These warmer regions are no longer solitary, as observed in previous decades, but they create long and linked thermal patterns.

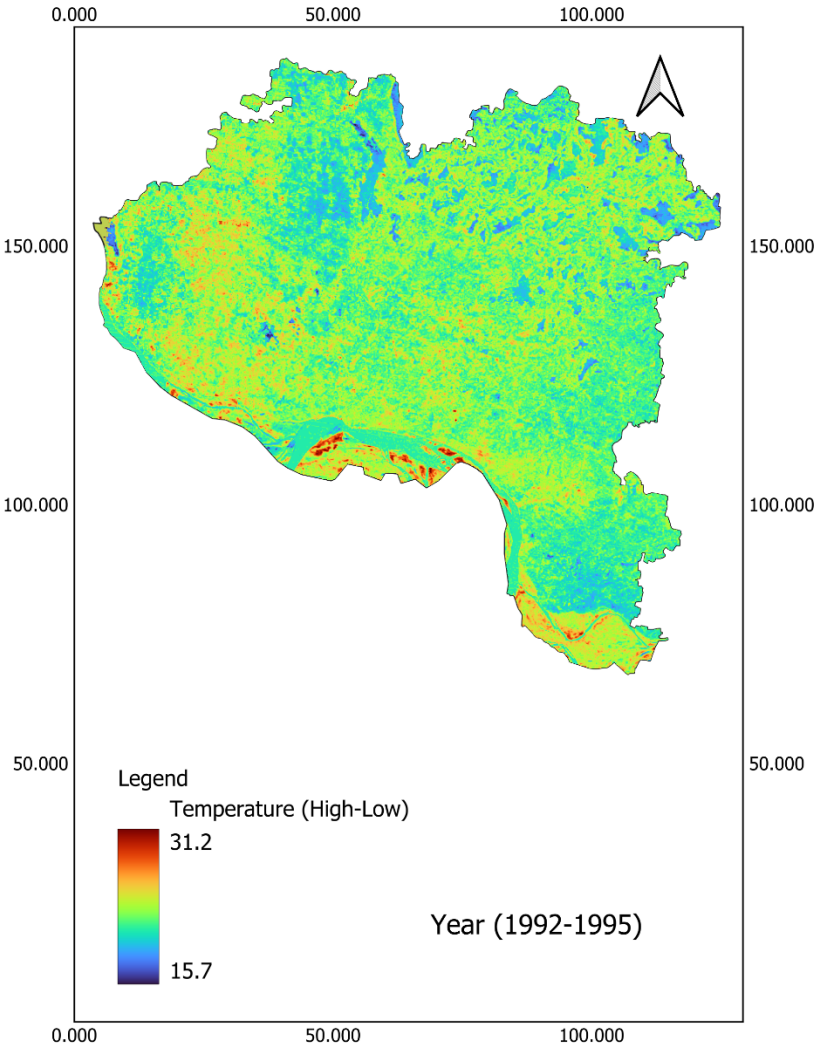

Fig.15. Spatiotemporal evolution of LST in Rajshahi district (1992–1995)

The interior agricultural landscapes are more characterised by surface temperature variability, where warm pockets are sprinkled and are embedded on moderately warm backgrounds. This trend indicates the increase in the intensity of land-atmosphere interactions, which are caused by agricultural activity, fluctuations in soil moisture, and surface exposure. Lower temperatures in the color blue and cyan indicate areas that remain cool, primarily around water bodies and small areas that have vegetation. Nevertheless, such cooling amenities seem to be more fragmented and space-bound, which means a decline in the ability to store heat on the district level. Altogether, the 1992-1995 years are a shift towards a district-wide surface warming, in which the spatial coverage of higher temperatures and the cool areas

is reduced. Global warming is indicated by the increase in high-temperature regions that induce long-term warming trends, which are still on the rise in later years.

- **Surface Temperature Distribution (1996–1999)**

The surface temperature distribution of the land surface in the period of 1996 to 1999 shows that the surface warming has increased further in the Rajshahi district. In comparison with the past era, warm temperature classes dominate more, and the green and yellow colors prevail in the interior landscape. The change indicates an overall increase in the base level temperature on agricultural and semi-natural surfaces. The regions of high temperature, which are represented by orange and red colors, grow significantly along the southern and southeastern boundaries of the district. The regions create an uninterrupted hotspot of thermal regions, especially around river confluences and low-lying floodplains, where bare soils and the sparsity of vegetation cover increase heat gain. The continuity of these hotspots indicates the existence of long-term warming and not brief thermal events.

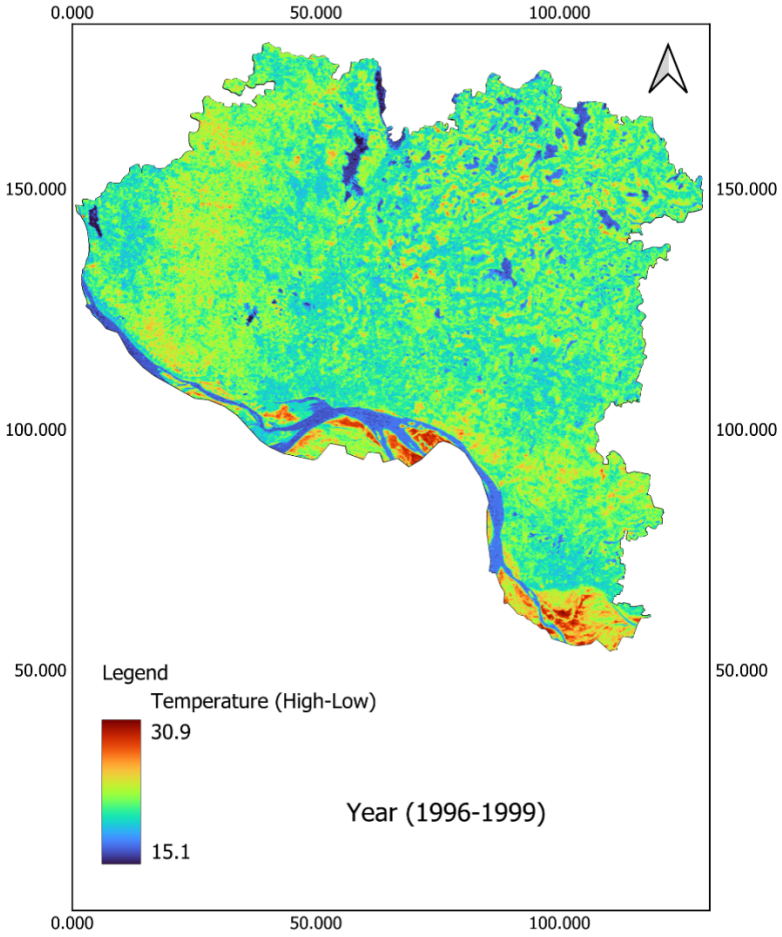

Fig.16. Spatiotemporal evolution of LST in Rajshahi district (1996–1999)

The spatial variability is observed to be higher in the central and western regions, and the warm patches and moderately warm patches are interspersed, which shows that the conditions of the land surface are not homogeneous. Though cooler zones can still be observed around large water bodies and drainage systems, their spatial scale has dwindled as compared to the past, and the cooling effect seems to have become more localized. To the north of the district, there are moderately warm conditions, with a reduced number of cool clusters compared to those experienced in the last few decades. Such a trend implies degradation of natural thermal buffering processes of the larger landscape. In general, the 1996-1999 period can be discussed as a significant period of transition to the process of lasting surface

warming in the Rajshahi district. The growth and maintenance of the high-temperature areas and the shrinkage of the cooler regions point out the growing exposure of the region to surface heat stress and other related climatic effects.

- **Surface Temperature Distribution (2000–2003)**

As can be seen in the 2000-2003 land surface temperature map, there is a definite increase in the intensity and spatial intricacy of surface warming within the Rajshahi district. There was an upward movement of the thermal baseline in the region, with moderately warm classes of temperature (green to yellow colors) becoming dominant in most parts of the district as compared to the late 1990s. The orange-red areas (areas with high temperature) become more and more concentrated along the riverine corridor to the south and the southeastern ends of the district. These hotspots are more fragmented yet more spatially concentrated, implying localized hotspots of heat related to bare floodplains, sandbars, and highly farmed agricultural lands. The fact that these hotspots persist along the riverbanks means that less evaporation cooling occurs and more surface energy is taken up.

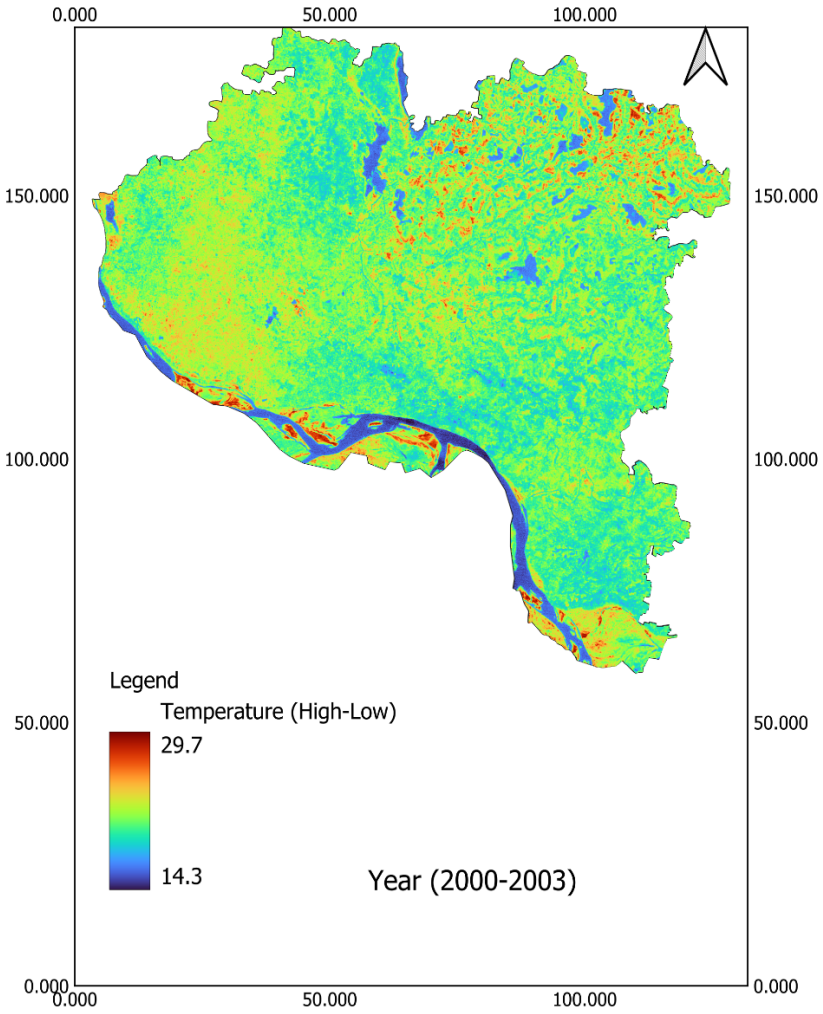

Fig.17. Spatiotemporal evolution of LST in Rajshahi district (2000–2003)

A decrease in thermal heterogeneity is apparent in the northern and northeastern regions, where there is an increasing incidence of warm patches mixed with fewer cool areas. The cooler surfaces (hues of blue) are mostly restricted to active riverbeds and water masses, but their spatial impact is thin and more and more interrupted. The relatively homogenous warm conditions of the western parts of the district, with little cool refuges, underscore the homogenization of the surface temperatures with time. This trend indicates a growing land-atmosphere interaction, probably caused by the intensification of land use and reduced vegetative cover. All in all, the years between 2000 and 2003 represent a crucial shift towards the continuous and spatially widespread surface warming in the Rajshahi

district. The growth of warm classes and the accumulation of thermal hotspots are indicators of increased vulnerability to heat stress, and would have consequences in terms of agricultural productivity, soil moisture depletion, and resiliency of regional climate.

- **Surface Temperature Distribution (2004–2007)**

The map of the 2004-2007 land surface temperature shows that there is further aggravation and spatial concentration of warming trends in the Rajshahi district. In comparison with the early 2000s, warm classes of temperature (yellow to light orange hues) are widespread in most of the interior areas, which is indicative of an ongoing increase in the average temperature of the surface. Hotspots of very high temperature (orange up to red color) are pronounced along the riverine belt towards the south and southwest, especially in the path of the main river and the floodplain lands along the river. These hotspots are continuous and spatially linked more than previously, implying the possibility of sustained heat release and not individual warming scenarios. There is also a high intensity of thermal in the southeastern region of the district, which means that it is getting more exposed to surface heat stress.

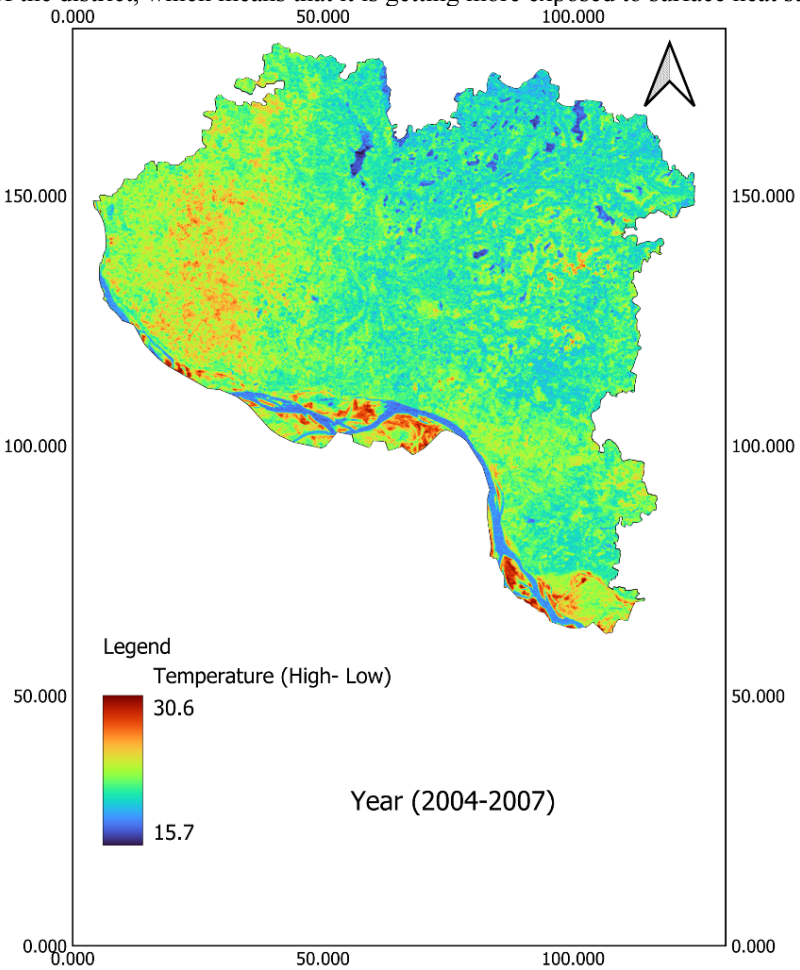

Fig.18. Spatiotemporal evolution of LST in Rajshahi district (2004–2007)

The western area is characterized by the significant growth of warmer regions, and the numbers of cold zones decrease. This standardization of temperature implies the combined reduction of the buffering capabilities of vegetation and soil moisture. Conversely, the northeastern and northern regions are relatively colder (green to blue colors); furthermore, the territories of cooler temperatures have become smaller than they were decades ago. Existing at low temperatures (blue colors) are also limited to the active river channels and water bodies, which underlines the importance of the surface water to cool local temperatures. Nonetheless, the small area imprints imply the shrinking ability of offsetting

regional warming. In general, the 2004 to 2007 season is a shift to a sustained and spatially widespread surface warming of the Rajshahi district. Continuous growth of thermal hotspots and the prevalence of warm temperature classes are indicative of growing susceptibility to the effects of heat on the environment, especially agriculture, water resources, and land management systems.

- **Surface Temperature Distribution (2008–2011)**

The 2008 to 2011 land surface temperature map shows that levels of surface warming increase intensely and extensively across the Rajshahi district. Large areas of the west and central regions are occupied by classes of warm temperature (yellow to orange), which is a clear indication of higher baseline surface temperatures than previously. There are two contrasting hot spots of high temperature (orange to reddish tones), which are highly concentrated in the northwest and west of the district. The density and continuity of high temperatures in these areas imply that there is continuous heating up that is probably due to the lack of vegetation cover, high agricultural activities, and depletion of soil moisture. The river-facing southwestern areas of the country also have long warm belts, which are indicative of increased thermal stress along floodplain areas and sandbar areas.

.

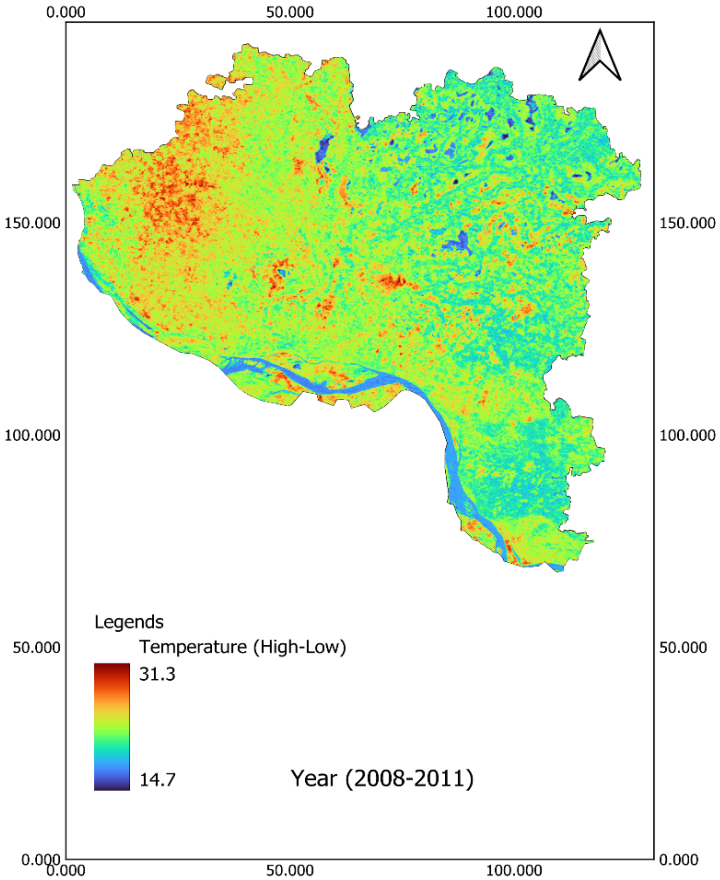

Fig.19. Spatiotemporal evolution of LST in Rajshahi district (2008–2011)

The middle and eastern areas portray an unequal distribution of hot and warm climates, with hotspots sparsely scattered on a more comprehensive background of green-yellow. This spatial heterogeneity implies that there is growing thermal variability with local land-use features and surface properties getting to control temperature distribution more firmly. It is a comparatively cooler surface (blue to cyan colors) that is seen along the major river

channels and water bodies, especially in the south and southeast corridors. These properties remain localized thermal buffers, but their effect seems to be reduced with a rise in the warming of the surrounding land areas. In general, the period from 2008 to 2011 is a serious period of enhanced surface warming in the Rajshahi district. The growing presence of high-temperature regions and the preeminence of warmer classes in the western and central regions indicate an increase in the condition of heat stress, which indicates the increased susceptibility of agricultural productivity, ecosystem stability, and the ability to withstand climate change in the region.

- **Surface Temperature Distribution (2012–2015)**

The 2012-2015 land surface temperature (LST) map reveals a further increase in warming in the Rajshahi district, which is a shift towards the localized hotspots towards more spatially integrated hot zones of high temperatures. The warm classes of temperature (yellow to orange colors) have become widespread in most parts of the district as compared to the past, which shows that the background temperatures of the surfaces have increased beyond the previous level. Hotspots of high temperature (orange and red colors) are evidently felt in the west and the northwest parts, where there are dense patterns of increased LST, indicating the buildup of heat. These regions are probably the complex interactions of high-level agricultural work, decreased vegetative cover in dry periods, and growing water stress on the soil. The high temperatures concentrated along the riverbanks, and the elongated belts of high temperatures are also observed in the southern floodplain and river-proximate regions, with markedly increased thermal sensitivity in these geomorphologically dynamic regions.

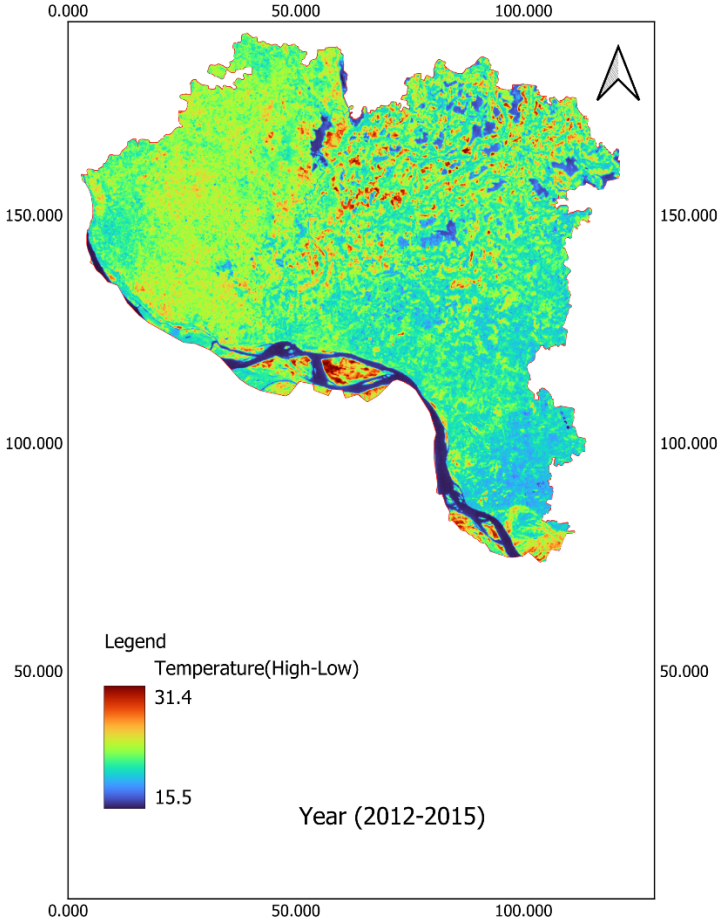

Fig.20. Spatiotemporal evolution of LST in Rajshahi district (2012–2015)

The core and the northeast areas of the district have a heterogeneous thermal pattern, with warm and moderate temperature spots in between. Such mosaic formations are signs of increasing spatial variability of surface heating with land use, crop cycles, and the surface moisture conditions becoming a larger modulator of the local temperature response. Relative lower temperatures (blue to cyan colours) continue along major riverways and water bodies,

particularly on the southern route. Their area of coverage, however, is seemingly less than in earlier decades, and this may indicate a diminished cooling effect in the wake of spreading regional warming. Generally, the 20122015 period has been characterized by a high level of surface warming in the Rajshahi district, where the intensity and the spatial distribution of the high-temperature regions have been registered significantly. This trend is an indicator of increased thermal stress to agricultural systems, water resources, and human settlements, and it supports the concern related to increased heat-associated risks in the context of a continuously changing climate.

- **Surface Temperature Distribution (2016–2019)**

With the 2016-2019 land surface temperature map, a very high increase in the intensity and the spatial continuity of high-temperature regions can be seen throughout the Rajshahi district. Warm temperature classes (yellow to orange colors) have made up a significant portion of the landscape since the previous decades, which displays a significant increase in the surface temperature at the posts. Extensive and continuous hotspots in the northwestern and western areas, with the orange to red patches gaining more spatial coherence. This trend indicates a long-term stressful condition of the thermo-regulation, most probably induced by low soil moisture, advanced agricultural activities, and low vegetative cooling in the long dry periods. These are seen to act as hotspots of the district.

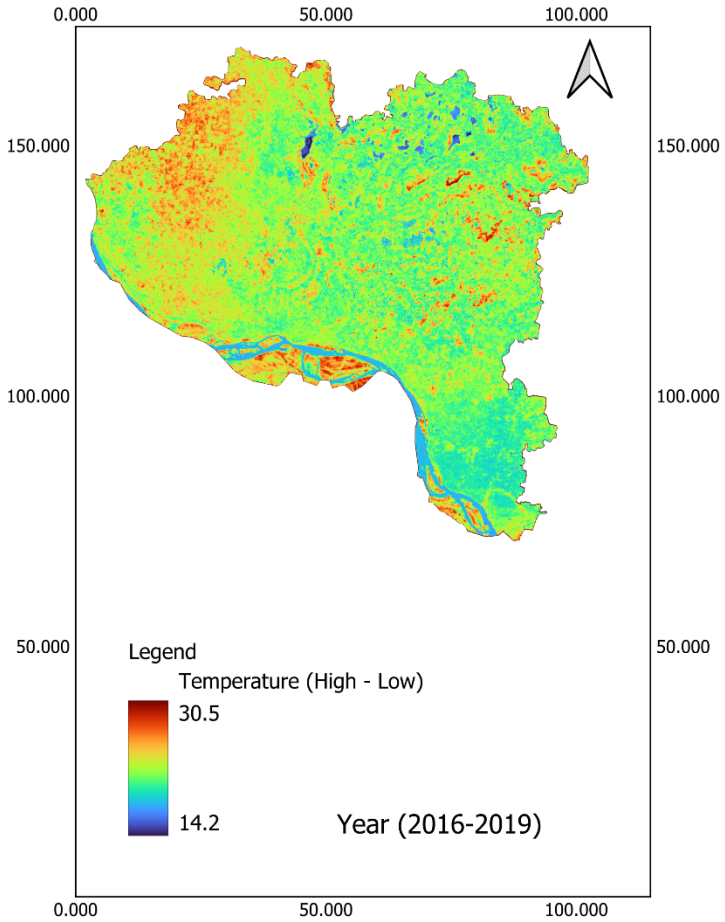

Fig.21. Spatiotemporal evolution of LST in Rajshahi district (2016–2019)

Bands of high temperatures are also evident along the southern corridor, and riverine floodplains formed most especially in the exposed riverbanks and sandbars. Though water channels manage to keep rather cooler temperatures (blue to cyan colors), their cooling effect is more and more localized and less effective to counteracting the heating of the surfaces surrounding. Such shrinkage of cooler areas is an indication of increased evapotranspiration and reduced availability of surface moisture. The core and northeast of Rajshahi are shown to have a high density of mosaic moderate-high temperature values, showing that there is high spatial variability of the surface heating. Such

heterogeneity is also an indicator of the increased impacts of land-use patterns, cropping intensity, and surface cover changes on the local thermal conditions. In general, the 2016-2019 interval is a more progressive phase of warmer temperatures on surfaces, which is marked by the prevalence of thermal hotspots and the lack of cooling shelters. Such conditions indicate growing susceptibility of agricultural systems and water quantity to heat pressure and support the newly arisen threat of drought-like circumstances in Rajshahi district..

- **Surface Temperature Distribution (2020–2024)**

The 2020-2024 map of the land surface temperature shows the greatest warming, which is spatially concentrated and takes place in the area of the district of Rajshahi throughout the entire time frame of the study. The areas with high temperature (orange and red colors) grow significantly in the northwestern and western regions of the district, creating large and continuous heat clusters. These areas are chronic thermal hotspots, meaning that it involves chronic surface heating instead of anomalies that occur in short-term or on a seasonal basis. The temperature of central Rajshahi is currently showing an overall increase in the temperate classes (from green to yellow), compared to the last several decades. Larger areas of cooler zones (blue colors) are restricted to river channels and immediate floodplain areas and the spatial coverage of these areas is significantly smaller. This implies that the natural cooling processes related to surface water are weakened and that stress in terms of evapotranspiration increases.

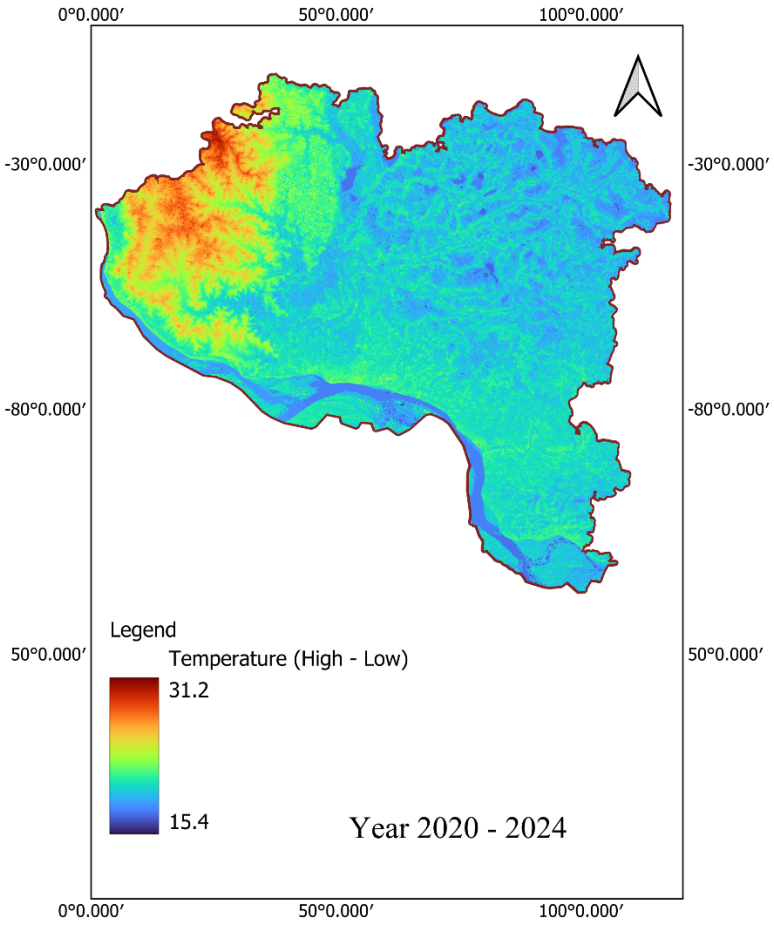

Fig.22. Spatiotemporal evolution of LST in Rajshahi district (2020–2024)

The corpus of the southern and southeastern corridors is characterized by long trains of high temperatures in fields in the riverbanks and on the nearby farmland. Those trends are in line with the exposure of sediments, the lack of soil moisture, and the increased land-atmosphere heat exchange in dry seasons. On the contrary, agricultural areas located inside that used to have mixed thermal conditions are now more homogenous with regard to warming. In general, the 2020-2024 period represents a higher level of thermal intensification in the Rajshahi district, where hotspots are evenly

distributed with large areas of accumulation of heat, and the coolers' refuges are shrunk, the coherent spaces of hotspots are more significant. These circumstances have direct effects on the development of droughts because the prolonged surface warming increases the demand for evapotranspiration, increases the rate of soil moisture depletion, and exposes agricultural systems to more vulnerability. The resulting spatial patterns are thus a good geospatial signal of the growing drought risk as predicted by the temperature forecasting models.

6. Implications for Agriculture and Climate Adaptation

The history of Bangladesh is marked by frequent droughts that have had a significant impact on the agricultural productivity and supply of water, especially in the northwestern part. The significant drought events of the past forty years (1971-2019) such as the severe droughts of 1982-1983, 1994-1995, 1997, 2000, and the 2014-2015 have contributed to the substantial decrease in the yield of rice and wheat, crop failure, and other socioeconomic effects as shown in Table 3 (FAO, 2007; Banglapedia, 2018). The recurring nature of the droughts in several decades is one indicator to show that drought in Bangladesh is not an incidental risk, but it is a structural climatic stressor integrated in the local climate framework. As depicted in Table 3, the northwestern part of Bangladesh, with Rajshahi district coming up as a regular drought hotspot, also indicates that the area is structurally weak to climatic extremes. The responses in the past to droughts were mainly reactive in nature, being more concerned with the relief and recovery after droughts instead of risk reduction. This responsive strategy led to repetitive agricultural failures, water scarcity, and food security problems, especially when it comes to smallholder agricultural systems that rely on climate-sensitive produce. The results of the current research have a high correlation with this historical trend and extend it to the perspective of future risks. The apparent increase in air temperature over the long term, a rapid growth in the occurrence of high-temperature outliers, and the systematic increase in the hotspots of land surface temperature (LST), in particular, in the western and southern agricultural belts of Rajshahi, are evidence that the risk of drought in the future is expected to escalate with the ongoing warming. Consistent heat stress enhances the speed of evapotranspiration, soil moisture, and the shortening of crop phenological stages, which diminishes the yield potential. Such effects are especially imperative to staple crops that are water-intensive, like rice, which constitute a major part of agricultural output in northwestern Bangladesh and have in the past experienced the most severe losses during recorded drought years, as shown in Table 3.

Table 3. Major drought events in Bangladesh and their agricultural impacts (1971–2019)

Year(s)	Affected Region	Key Impacts	Reference
1971	Nationwide	Severe drought compounded by socio-political instability	Hossain (2003)
1980	Northern Bangladesh	Major agricultural disruption	Mian & Hossain (1984)
1982–1983	Northwestern Bangladesh	Severe crop failure and economic loss	Islam & Karim (1985)
1994–1995	Northwestern Bangladesh	Persistent drought; major rice and jute losses	Rahman & Khan (1995)
1997	Large parts of Bangladesh	Widespread crop yield reduction	Chowdhury (1998)
2000	Northern Bangladesh	Significant rice and wheat production decline	Khan & Chowdhury (2001)
2006	Northwestern Bangladesh	25–30% reduction in Aman rice production	FAO (2007)
2009	Northern Bangladesh	Water shortages and productivity decline	Mollah (2010)

Year(s)	Affected Region	Key Impacts	Reference
2014–2015	Multiple regions	Severe drought affecting agriculture and water availability	Haque & Ahmed (2015); Islam (2016)
2019	Nationwide	Significant agricultural and economic impacts	Sarker & Rahman (2020)

Source: FAO (2007); Banglapedia (2018)

In this vein, the AI-GIS framework developed as part of the current study is a crucial step to agricultural planning and climate adaptation. The combination of long-horizon temperature forecasting (up to 2034) with spatially explicit heat stress mapping can facilitate the proactive recognition of developing drought risk zones by the framework before they experience severe impacts.

This capability supports:
(i)the irrigation infrastructure and water management investments in the continuously heat-stressed localities should be prioritized;
(ii) identification of vulnerable agricultural areas to climate, which must be targeted by intervention;
(iii) encouragement of climate-appropriate crop and variety selection, such as those drought- and heat-tolerant crops; and
(iv)empowerment of drought early-warning mechanisms by predictive identification of thermal stress.

Notably, the overlap between past drought effects recorded in Table 3 and the warming and spatial heat responses projected in the study suggests that future drought effects could be predicted rather than responding once they have occurred, when damages have already been incurred. By transforming past experiences of drought into practical intelligence for climate management, the proposed framework enables the conversion of a reactive response to drought to proactive climate risk management. This shift is necessary in order to minimize future agricultural losses, improve food security, and create long-term climate resilience in Bangladesh as well as other agrarian areas susceptible to drought.

7. Discussion

The results of this paper show that signal decomposition methods, when combined with advanced machine learning architectures, offer a powerful system of long-term temperature prediction in areas with drought. The nonlinear and non-stationary features of temperature time series were well represented using hybrid models because they did not depend on learning to identify intrinsic components before predicting, leading to better predictive stability and accuracy. The effectiveness of decomposition-based methods was always superior to that of individual statistical and deep learning models, which proved that the variability of temperatures in northwestern Bangladesh is under the control of the multi-scale processes and long-term persistence. These findings highlight the need to preprocess climatic signals in the use of artificial intelligence to climate forecasting and impact assessment. According to long-term temperature forecasts, the Rajshahi district is projected to experience continuous warming during the 2030s, which is accompanied by the growing number of high-temperature anomalies and a change in the location of decadal temperature distributions towards the warmer side. The expansion of upper percentiles of temperature indicates the increase of exposure to extreme heat conditions that have a direct effect on the evapotranspiration demand and surface moisture loss. This is because the consistent pattern in the warming of various hybrid models is a good indicator that the observed pattern is a good climatic message and not a model artifact. The spatial trends of the predicted warming trends are based on the spatial evidence that is offered by spatiotemporal analysis of the Landsat-derived land surface temperature. Several initial decades had more homogeneous and moderate surface temperatures, and the recent times are marked by extensive growth and development of thermal hotspots. Long spells of high temperatures are especially

noticeable in western and southern agrarian areas of Rajshahi, and colder surfaces are becoming more concentrated in the slender river courses and water bodies. This is a shrinking of the cooling refuges in space, which is an indication of a degrading natural thermal buffering power, and which posits a change in small-scale anomalies in heat to widespread surface warming throughout the district. Available historical records of droughts indicate that Bangladesh, and particularly its northwestern part, has witnessed frequent and severe droughts during the last five decades, with massive losses both in terms of agriculture and the economy. The intersection of these historical patterns of drought with the projected patterns of warming in the study point to a high probability that the effect of drought risk will increase with further increases in temperature. Nevertheless, as opposed to the previous methods of drought management, which were mostly reactive, the integrated AI-GIS framework that was created in this study can allow for to detection of the development of drought stress early. The framework is able to predict the future surface temperature trajectories and map persistent surface heat stress to create forward-looking climate risk intelligence out of past drought experience. This has far-reaching consequences to agriculture and climate adaptation. Repeated exposure to heat stress may increase the phenological speed, de-escalate the growth cycles, and cause low yields, especially in water-guzzlers like rice, which constitute the bulk of agricultural production in northwestern Bangladesh. Higher evapotranspiration needs during a rise in temperature increase the needs of irrigation, which further puts strain on already limited water resources. The proposed framework, through integrating the long-horizon temperature prediction with the spatial heat exposure mapping, assists in active decisions, such as the priorities in the irrigation infrastructure, the susceptibility of agricultural areas to climate change, the utilization of drought- and heat-resistant plant species, and the improvement of drought early warning systems. This combination of temporal and spatial enables the transition of crisis response to proactive risk management of climatic conditions, which is needed to enhance food security and agricultural resilience. Altogether, as shown in this study, hybrid artificial intelligence models with long-term satellite-based geospatial analysis is a scalable and useful solution to evaluating climate-driven drought risk in data-constrained areas. The proposed AI-GIS framework takes the future temperature forecasting and spatial patterns of heat stress and relates them to the conditions of the historical drought to enhance drought early-warning capabilities, as well as climate adaptation planning. The results have practical implications for sustainable agricultural management in Bangladesh, which can be applied to other agrarian systems that are sensitive to global climate change and experiencing the threat of rising droughts.

8. Limitations and Future Research Directions

Although this paper has presented a complete evaluation of the drought risk due to temperature variations through a combined AI-GIS platform, it is important to note that the study has some limitations. First of all, analysis is centered on air temperature and land surface temperature because the stress factors of drought depend on these factors. Even though temperature is the leading factor in evapotranspiration and drying of the surface in semi-arid areas, drought is a complex process of factors determined by the variability of precipitation, dynamics of soil water, the presence of groundwater, and the vegetation reactions. These variables might not be included, and this may confine the capability of complete characterization of hydrological and agricultural drought processes. Second, the prediction model is based on past climatic trends that can determine future climatic trends. Although multiple hybrid models are robust, long-term climate predictions are always uncertain, especially in the changing land-use conditions and the changing atmospheric circulation patterns. The ensemble-based and probabilistic forecasting methods might help to alleviate the uncertainty and enhance the trust in long-period projections. Third, the projected thermal stress in this study is not explicitly associated with crop yield and socioeconomic implications. Even though land surface temperature and air temperature are strong proxies of agricultural stress due to drought, combining crop simulation models with yield datasets would make it possible to assess more readily the productivity loss and food security consequences. The further study ought to incorporate the framework with multi-variable hydroclimatic data, which include precipitation, soil moisture, and evapotranspiration to vegetation indices to create a more comprehensive drought assessment system. Connecting the AI -GIS model to crop development models and socioeconomic indicators would also make the model more relevant in agricultural planning and policy development. Also, the framework application on several climatic

territories and scales would assist in assessing its generalizability and contribute to the climate-wide adaptation and drought-resistance efforts.

9. Conclusion

This paper has created a coupled artificial (Gyaneshwar et al., 2023)l intelligence-geospatial model to evaluate long term and climate temperature changes, spatial heat stress and agricultural risk during drought in the Rajshahi district, a climate-prone area in Bangladesh. The framework could be used to predict the nonlinear and non-stationary dynamics of the temperature time series and make reliable temperature projections up to 2034 by applying advanced signal decomposition algorithms with machine learning and deep learning models. The excellent result of the hybrid decomposition-based models shows that they are suitable in data-limited scenarios with long-horizon climate prediction. The findings indicate that there has been a consistent warming pattern with the number of high-temperature aberrations on the rise. The systematic growth and increase in the extent of thermal hotspots, especially in the western and southern agricultural areas can also be seen in multi-decadal examination of Landsat based land surface temperature. The overlap of the patterns of air temperature change on the one hand with the patterns of observed surface warming on the other one is a strong indicator of increasing heat stress and drought vulnerability in the area. Combining the time prediction with the exposure map of the spatial information, the proposed AI/GIS network provides the proactive drought risk assessment and farm planning approach. The capacity to detect the developing drought-prone areas, and to institute the necessary adaptation strategies, such as the better irrigation control, selection of climate-ostensible crops, and drought early warning mechanisms, is justified. Notably, the framework helps in changing the reactive response to droughts to proactive management of climatic risks that are essential in improving food security and resilience of agrarian systems facing droughts. In general, this paper indicates that AI-GIS hybrid solutions can offer feasible climate intelligence to support sustainable agricultural management and climate adaptation. The suggested framework is scalable and transferable, which is not only valuable in practical terms to Bangladesh but also to other climate sensitive areas that are at the threat of rising drought owing to the current climate change.

Author Contributions.

Hasan Ahamed Alif was the brainchild and designer of the study, the general framework of the research, and the overall head of the integration of artificial intelligence and geospatial approaches. He carried out data acquisition and pre-processing, actualized the hybrid machine learning models, statistical analysis, and GIS-based analysis, and analyzed the data. The original manuscript was prepared by Hasan Ahamed Alif, and the revision and finalization were headed by Alif. Data processing, model validation, and performance evaluation were done by Md. Jisan Mashrafi. He helped with the execution of the experiment with machine learning, the interpretation of results, and assisted in the preparation and technical review of figures and tables. Sudoy Kumer Ghosh contributed to the literature review, contextual analysis of the effects of drought, and interpretation of the implications of the adaptation of agriculture and climate. He helped in the editing of the manuscripts, refinements of the discussion parts, and improvement of the final manuscript. The final manuscript was reviewed and approved by all authors.

Acknowledgments

The authors owe a debt of gratitude to the Bangladesh Meteorological Department (BMD) to assisting in this study by supplying them with long-term temperature information. The authors also recognize the United States Geological Survey (USGS) and NASA as the ones that made Landsat satellite data publicly available, and Google Earth Engine as the service offering an effective cloud-based platform to compute and analyze geospatial data. The authors are appreciative of the helpful discussions and informal feedback provided to them by academic peers and mentors that helped them to produce a better and more understandable piece of work. This research did not get any specific funding. The authors also reveal that Grammarly, QuillBot, and Consensus are artificial intelligence-based tools that were employed to help in language refinement, grammar fix, and exploration of literature. These tools were applied only in

order to enhance clarity and readability. It is up to the authors to do all scientific content, analysis, interpretations, and conclusions.

Funding Information

In this study, no funding was obtained.

Conflict of interest declaration

There is no conflict of interest that the work poses to the author.

Availability of data statement

All the datasets that were examined in this study can be accessed by the author through a reasonable request.

Statement of Novelty

The paper presents a combined structure of artificial intelligence and geospatial systems that combines the power of an upgraded hybrid machine learning model and multi-decadal satellite-derived land surface temperature data to evaluate the risk of droughts caused by the temperature factor. This study is an explicit couple of predictive air temperature forecasting and spatiotemporal land surface temperature in contrast to the earlier researches, which consider long-term temperature forecasting and spatial heat stress assessment as different hypotheses. The research provides a step forward in drought early-warning research by working with the hybrid models based on signal decomposition and long-horizon data forecasting in an area that is limited in data and at risk of climate, as well as by correlating the past drought experience with future climate predictions. The framework that is suggested is a new, scalable, and transferable method of active drought risk analysis and climate adaptation planning.

Statement of Industrial Relevance

The results of this paper are directly applicable in the agricultural industries, management of water resources, and decision-making processes with respect to climate. The combined AI-GIS system will be able to assist irrigation authorities, agricultural planners, and climate-service providers in finding the areas at risk of drought and streamlining water allocation plans in the field of growing thermal stress. The framework can be used to support climate-sensitive agricultural activities, crop choice, and infrastructure investment by providing early warning of the risk of drought caused by temperature variations to minimize losses in the economy and improve agricultural resilience. The method can be applied to existing drought surveillance applications, agri-technology, and climate risk evaluation applications, which would provide viable value to the public and non-governmental stakeholders in climate-dependent sectors.

Reference

Ayadi, R., Forouheshfar, Y., & Moghadas, O. (2025a). Enhancing system resilience to climate change through artificial intelligence: A systematic literature review. *Frontiers in Climate*, *7*, 1585331. https://doi.org/10.3389/fclim.2025.1585331

Ayadi, R., Forouheshfar, Y., & Moghadas, O. (2025b). Enhancing system resilience to climate change through artificial intelligence: A systematic literature review. *Frontiers in Climate*, *7*, 1585331. https://doi.org/10.3389/fclim.2025.1585331

Barzigar, A., Allahyari, S., Fathi, M., Mujumdar, A. S., & Hosseinalipour, S. M. (2025). Modeling freshwater yield: Deep learning applications in seawater greenhouses in Iran. *Scientific Reports*, *15*(1), 36647. https://doi.org/10.1038/s41598-025-20548-y

Biazar, S. M., Golmohammadi, G., Nedhunuri, R. R., Shaghaghi, S., & Mohammadi, K. (2025a). Artificial Intelligence in Hydrology: Advancements in Soil, Water Resource Management, and Sustainable Development. *Sustainability*, *17*(5), 2250. https://doi.org/10.3390/su17052250

Biazar, S. M., Golmohammadi, G., Nedhunuri, R. R., Shaghaghi, S., & Mohammadi, K. (2025b). Artificial Intelligence in Hydrology: Advancements in Soil, Water Resource Management, and Sustainable Development. *Sustainability*, *17*(5), 2250. https://doi.org/10.3390/su17052250

Birant, K. U., Ghasemkhani, B., Varlıklar, Ö., & Birant, D. (2025). A new machine learning method for rainfall classification: Temporal random tree. *PeerJ Computer Science*, *11*, e3022. https://doi.org/10.7717/peerj-cs.3022

Cho, K., van Merrienboer, B., Gulcehre, C., Bahdanau, D., Bougares, F., Schwenk, H., & Bengio, Y. (2014). *Learning Phrase Representations using RNN Encoder-Decoder for Statistical Machine Translation* (Version 3). arXiv. https://doi.org/10.48550/ARXIV.1406.1078

Dragomiretskiy, K., & Zosso, D. (2014). Variational Mode Decomposition. *IEEE Transactions on Signal Processing*, *62*(3), 531–544. https://doi.org/10.1109/TSP.2013.2288675

Guo, Q., He, Z., Wang, Z., Qiao, S., Zhu, J., & Chen, J. (2024). A Performance Comparison Study on Climate Prediction in Weifang City Using Different Deep Learning Models. *Water*, *16*(19), 2870. https://doi.org/10.3390/w16192870

Han, H., Liu, Z., Li, J., & Zeng, Z. (2024). Challenges in remote sensing based climate and crop monitoring: Navigating the complexities using AI. *Journal of Cloud Computing*, *13*(1), 34. https://doi.org/10.1186/s13677-023-00583-8

Hanadé Houmma, I., El Mansouri, L., Gadal, S., Garba, M., & Hadria, R. (2022a). Modelling agricultural drought: A review of latest advances in big data technologies. *Geomatics, Natural Hazards and Risk*, *13*(1), 2737–2776. https://doi.org/10.1080/19475705.2022.2131471

Hanadé Houmma, I., El Mansouri, L., Gadal, S., Garba, M., & Hadria, R. (2022b). Modelling agricultural drought: A review of latest advances in big data technologies. *Geomatics, Natural Hazards and Risk*, *13*(1), 2737–2776. https://doi.org/10.1080/19475705.2022.2131471

Hochreiter, S., & Schmidhuber, J. (1997). Long Short-Term Memory. *Neural Computation*, *9*(8), 1735–1780. https://doi.org/10.1162/neco.1997.9.8.1735

Huang, G.-B., Zhu, Q.-Y., & Siew, C.-K. (2006). Extreme learning machine: Theory and applications. *Neurocomputing*, *70*(1–3), 489–501. https://doi.org/10.1016/j.neucom.2005.12.126

İşler, B. (2025). Evaluating urbanization effects on biomass density using a hybrid AI model: A case study. *Scientific Reports*, *15*(1), 34932. https://doi.org/10.1038/s41598-025-18750-z

Jang, J.-S. R. (1993). ANFIS: Adaptive-network-based fuzzy inference system. *IEEE Transactions on Systems, Man, and Cybernetics*, *23*(3), 665–685. https://doi.org/10.1109/21.256541

Kingma, D. P., & Ba, J. (2014). *Adam: A Method for Stochastic Optimization* (Version 9). arXiv. https://doi.org/10.48550/ARXIV.1412.6980

Le Roux, M., Kunert, K. J., Cullis, C. A., & Botha, A. (2024a). Unlocking Wheat Drought Tolerance: The Synergy of Omics Data and Computational Intelligence. *Food and Energy Security*, *13*(6), e70024. https://doi.org/10.1002/fes3.70024

Le Roux, M., Kunert, K. J., Cullis, C. A., & Botha, A. (2024b). Unlocking Wheat Drought Tolerance: The Synergy of Omics Data and Computational Intelligence. *Food and Energy Security*, *13*(6), e70024. https://doi.org/10.1002/fes3.70024

LeCun, Y., Bengio, Y., & Hinton, G. (2015). Deep learning. *Nature*, *521*(7553), 436–444. https://doi.org/10.1038/nature14539

Liu, Z., Zhou, J., Yang, X., Zhao, Z., & Lv, Y. (2024). Research on Water Resource Modeling Based on Machine Learning Technologies. *Water*, *16*(3), 472. https://doi.org/10.3390/w16030472

McKinney, W. (2010). *Data Structures for Statistical Computing in Python*. 56–61. https://doi.org/10.25080/Majora-92bf1922-00a

Mokhtar, A., Jalali, M., He, H., Al-Ansari, N., Elbeltagi, A., Alsafadi, K., Abdo, H. G., Sammen, S. Sh., Gyasi-Agyei, Y., & Rodrigo-Comino, J. (2021). Estimation of SPEI Meteorological Drought Using Machine Learning Algorithms. *IEEE Access*, *9*, 65503–65523. https://doi.org/10.1109/ACCESS.2021.3074305

Ougahi, J. H., & Rowan, J. S. (2025). Enhanced streamflow forecasting using hybrid modelling integrating glacio-hydrological outputs, deep learning and wavelet transformation. *Scientific Reports*, *15*(1), 2762. https://doi.org/10.1038/s41598-025-87187-1

Parasar, P., Moral, P., Srivastava, A., Krishna, A. P., Sharma, R., Rathore, V. S., Mustafi, A., Mishra, A. P., Hasher, F. F. B., & Zhran, M. (2025). TeaNet: An Enhanced Attention Network for Climate-Resilient River Discharge Forecasting Under CMIP6 SSP585 Projections. *Sustainability*, *17*(9), 4230. https://doi.org/10.3390/su17094230

Pokhariyal, S., Patel, N. R., & Govind, A. (2023). Machine Learning-Driven Remote Sensing Applications for Agriculture in India—A Systematic Review. *Agronomy*, *13*(9), 2302. https://doi.org/10.3390/agronomy13092302

Qiao, X., Zhang, K., & Huang, W. (2025). Impacts of Climate Change on Oceans and Ocean-Based Solutions: A Comprehensive Review from the Deep Learning Perspective. *Remote Sensing*, *17*(13), 2306. https://doi.org/10.3390/rs17132306

Savitzky, Abraham., & Golay, M. J. E. (1964). Smoothing and Differentiation of Data by Simplified Least Squares Procedures. *Analytical Chemistry*, *36*(8), 1627–1639. https://doi.org/10.1021/ac60214a047

Schuster, M., & Paliwal, K. K. (1997). Bidirectional recurrent neural networks. *IEEE Transactions on Signal Processing*, *45*(11), 2673–2681. https://doi.org/10.1109/78.650093

Shahriar, S. A., Choi, Y., & Islam, R. (2025). Advanced Deep Learning Approaches for Forecasting High-Resolution Fire Weather Index (FWI) over CONUS: Integration of GNN-LSTM, GNN-TCNN, and GNN-DeepAR. *Remote Sensing*, *17*(3), 515. https://doi.org/10.3390/rs17030515

Smith, J. S. (2005). The local mean decomposition and its application to EEG perception data. *Journal of The Royal Society Interface*, *2*(5), 443–454. https://doi.org/10.1098/rsif.2005.0058

Subramaniam, S., Raju, N., Ganesan, A., Rajavel, N., Chenniappan, M., Prakash, C., Pramanik, A., Basak, A. K., & Dixit, S. (2022). Artificial Intelligence Technologies for Forecasting Air Pollution and Human Health: A Narrative Review. *Sustainability*, *14*(16), 9951. https://doi.org/10.3390/su14169951

Torres, M. E., Colominas, M. A., Schlotthauer, G., & Flandrin, P. (2011). A complete ensemble empirical mode decomposition with adaptive noise. *2011 IEEE International Conference on Acoustics, Speech and Signal Processing (ICASSP)*, 4144–4147. https://doi.org/10.1109/ICASSP.2011.5947265

Vapnik, V. N. (2000). *The Nature of Statistical Learning Theory*. Springer New York. https://doi.org/10.1007/978-1-4757-3264-1

Zellou, B., El Moçayd, N., & Bergou, E. H. (2023a). Review article: Towards improved drought prediction in the Mediterranean region – modeling approaches and future directions. *Natural Hazards and Earth System Sciences*, *23*(11), 3543–3583. https://doi.org/10.5194/nhess-23-3543-2023

Zellou, B., El Moçayd, N., & Bergou, E. H. (2023b). Review article: Towards improved drought prediction in the Mediterranean region – modeling approaches and future directions. *Natural Hazards and Earth System Sciences*, *23*(11), 3543–3583. https://doi.org/10.5194/nhess-23-3543-2023

Zhou, H., Zhang, S., Peng, J., Zhang, S., Li, J., Xiong, H., & Zhang, W. (2021). Informer: Beyond Efficient Transformer for Long Sequence Time-Series Forecasting. *Proceedings of the AAAI Conference on Artificial Intelligence*, *35*(12), 11106–11115. https://doi.org/10.1609/aaai.v35i12.17325

Bishop, C. M. (2006) *Pattern Recognition and Machine Learning*. New York: Springer.https://link.springer.com/book/9780387310732

Granville Tunnicliffe Wilson, 2016. "Time Series Analysis: Forecasting and Control, 5th Edition , by George E. P. Box , Gwilym M. Jenkins , Gregory C. Reinsel and Greta M. Ljung , 2015 . Published by John Wiley and Sons Inc. , Hoboken, N," Journal of Time Series Analysis, Wiley Blackwell, vol. 37(5), pages 709-711, September.

Cleveland, R. B.. "STL : A Seasonal-Trend Decomposition Procedure Based on Loess." (1990).https://api.semanticscholar.org/CorpusID:64570714

Ingrid Daubechies. 1992. Ten lectures on wavelets. Society for Industrial and Applied Mathematics, USA. https://dl.acm.org/doi/10.5555/130655

Hyndman, R.J., & Athanasopoulos, G. (2018) *Forecasting: principles and practice*, 2nd edition, OTexts: Melbourne, Australia. OTexts.com/fpp2

Mian, M. A., & Hossain, M. (1984). Agricultural impacts of drought in Bangladesh. Bangladesh Journal of Agricultural Research, 9(2), 1-10.

Hossain, M. (2003). Drought in Bangladesh: A historical perspective. Journal of Bangladesh Studies, 5(1), 1-15.

Islam, M. S., & Karim, Z. (1985). Drought and its impacts on the economy of Bangladesh. Journal of Bangladesh Studies, 7(1), 1-12.

Rahman, M. M., & Khan, M. A. (1995). Drought impacts on agriculture in Bangladesh. Bangladesh Journal of Agricultural Economics, 18(2), 1-10.

Chowdhury, A. M. (1998). Drought and its impacts on water resources in Bangladesh. Journal of Water Resources Management, 12(3), 1-15.

Khan, M. R., & Chowdhury, A. M. (2001). Drought and its impacts on agriculture in Bangladesh. Journal of Bangladesh Studies, 3(1), 1-10.

Mollah, A. R. (2010). Drought and its impacts on agriculture in Bangladesh. Journal of Bangladesh Agricultural University, 8(2), 1-10.

Haque, M. A., & Ahmed, M. (2015). Drought and its impacts on water resources in Bangladesh. Journal of Water Resources Management, 29(4), 1-12

Islam, M. S. (2016). Drought and its impacts on agriculture in Bangladesh. Journal of Bangladesh Studies, 18(1), 1-10.

Sarker, M. A. R., & Rahman, M. M. (2020). Drought and its impacts on agriculture in Bangladesh. Journal of Bangladesh Agricultural University, 18(2), 1-10.

FAO. (2007). Drought in Bangladesh: A historical perspective. Food and Agriculture Organization of the United Nations.

Banglapedia. (2018). Drought in Bangladesh. National Encyclopedia of Bangladesh.